Hydraulics Research
Wallingford

A LINEAR ARRAY FOR MEASURING DIRECTIONAL WAVE SPECTRA

R W P May

Report No SR 25
February 1985

Registered Office: Hydraulics Research Limited,
Wallingford, Oxfordshire OX10 8BA.
Telephone: 0491 35381. Telex: 848552

This report describes work carried out under contract DGR 465/33, "Wave propagation with application to port design" funded by the Department of Transport to 31 March 1984 and thereafter by the Department of the Environment. The departmental nominated officer at report date was Dr R P Thorogood, CIRU. The study was carried out by Mr R W P May in the Maritime Engineering Department of Hydraulics Research. Dr S W Huntington, Head, Maritime Engineering Department, was the Company's nominated project officer. This report is published on behalf of the Department of the Environment but any opinions expressed are not necessarily those of the Department.

ABSTRACT

The degree of protection provided by a harbour is different for short-crested waves than for long-crested ones. Good field data on the directional properties of real seas are therefore needed when designing harbours by means of physical or mathematical models. This report describes research, commissioned by the Department of Transport and the Department of the Environment, on a new method of measuring directional wave spectra at coastal sites.

The new method uses measurements of wave height provided by a linear array of gauges. The distances between adjacent probes are multiples of a unit spacing d, and are chosen so that a full set of spacings from d to (N-1)d is obtained by considering all possible pairs of gauges in the array. The value of N depends upon the number of gauges used and directly affects the angular resolution of the array.

The frequency spectrum of the waves recorded by each probe is determined and used to calculate the cross-spectra between all possible gauge pairs in the array. Suitably combining the values of the cross-spectra then gives direct estimates of the wave energy distribution at discrete angular intervals. The method therefore differs from some previous techniques which depend upon re-constructing the directional spectrum from a limited number of Fourier components of the angular distribution. The angular resolution of the linear array depends upon the number of gauge spacings, and also upon the unit spacing, d, and the wavelength of the waves being measured. Since the probes are arranged in a line, the array cannot differentiate between waves approaching from opposite directions. It is not therefore suitable for general use in the open sea, but can be used at coastal sites where the range of wave directions does not exceed 180°.

The method was tested in the Offshore Sea Basin at Hydraulics Research using one array with 5 probes and another with 9 probes and the same unit spacing. Five types of directional spectrum were measured in the experiments, and the results demonstrated the validity of the new technique. Although the larger array gave three times as many estimates of the angular distribution, the individual values tended to be more variable than those from the smaller array. The results of the tests suggest that a 6-gauge array should normally provide a sufficient amount of directional information.

The new technique is suitable for measurements at coastal sites, and could be adapted for use with pressure gauges mounted on the seabed. In water of 20m depth a 6-gauge array with a unit spacing of d = 20m would have an angular resolution of 6° for waves with a period of 6 seconds and 24° for waves of 16 seconds period.

SYMBOLS

A_n	Normalising constant in angular spreading function
a	Wave amplitude
$C_n(\omega)$	Real part of normalised cross-spectrum
D	Constant in equation (28)
d	Unit distance for spacings in linear array
E	Constant in equation (43)
F_i	Transfer function for output i
$f(\omega, \theta)$	Directional spreading function based on wave direction
G_m	Estimator for $g(\omega,k_2)$ defined by equation (40)
g	Acceleration due to gravity
$g(\omega,k_2)$	Directional spreading function based on wavenumber
h	Depth of water
I_r	Integral defined by equation (34)
J_r	Integral defined by equation (47)
K	Maximum value of k_2 in directional spectrum
k	Wavenumber

SYMBOLS (Cont/d)

k_1	*Component of k in x-direction*
k_2	Component of k in y-direction
M	Number of gauges in linear array
m	Integer variable
N	Number of different spacings in linear array (including zero)
n	Integer variable
P(X)	Function defined by equation (23)
$Q_n(\omega)$	Imaginary part of normalised cross-spectrum
r	Integer (= 2N-1)
$S_I(\omega)$	One-dimensional spectral density
$S_{II}(\omega,k_2)$	Two-dimensional spectral density based on wavenumber
$S_{II}(\omega,\theta)$	Two-dimensional spectral density based on wave direction
$S_{ij}(\omega)$	Spectrum of output signal i
$S_{ij}(\omega)$	Cross-spectrum of output signals i and j
$S_n(\omega)$	Cross-spectrum between two gauges distance n units apart
$T_m(\omega)$	Discrete transform defined by equation (17)

SYMBOLS (Cont/d)

t	Time
U	Limit of u in integration
u	Quantity defined by equation (31b)
x	Horizontal co-ordinate; axis parallel to centreline of basin
y	Horizontal co-ordinate; axis perpendicular to centreline of basin
z	Vertical co-ordinate
α	Quantity defined by equation (31c)
η	Elevation of free surface above mean water level
θ	Angular direction of wave propagation
ϕ	Phase angle
ω	Radian
$*$	Complex conjugate
$\hat{1}$	Estimated value

CONTENTS

TABLE

FIGURES

1 INTRODUCTION

Current methods of designing and testing harbours normally assume that the incident waves are long-crested. However, it has become clear that the short-crested nature of real seas needs to be taken into account when determining the degree of protection which a harbour will provide. Short-crestedness affects the amount of disturbance produced inside a harbour both by the primary waves and also by the longer period oscillations which are caused by wave grouping. Good field data on the directional distribution of wave energy near coasts is thus needed for use in both physical and mathematical models of harbours. This report is the second stage of a research programme on methods of measuring directional wave spectra which is being carried out at Hydraulics Research (HR) with funding provided by the Department of Transport and the Department of the Environment.

The first stage of this programme consisted of an experimental comparison of three "simple" gauges that are able to measure the mean direction and spread of wave spectra. The theoretical and experimental details of the study were described in a report by May [4], which will hereafter be referred to as Ref A. Each of the simple gauges measures three separate pieces of information about the wave field, and from this it is possible to determine the first two complex Fourier coefficients of the directional spectrum. Conventional methods for reconstructing the directional spectrum (see A) assume that the unknown higher-order Fourier coefficients are equal to zero; this leads to poor angular resolution particularly for waves that are closely concentrated about the mean direction. So-called data adaptive techniques such as the Maximum Likelihood Method (MLM), see Capon [1], are claimed to give better directional resolution from a limited amount of data. However, the theoretical basis of these techniques is not clear (see Gilbert [3] for a discussion of the MLM), and they do not always give consistent results.

A more accurate reconstruction of a directional spectrum can be obtained by determining a larger number of the Fourier coefficients. This in turn requires more independent measurements of the wave field. One example of this approach is provided by the NIO Cloverleaf buoy [2] which measured wave height, two wave-slopes and two wave curvatures. Another example is the circular array of wave height probes considered in A. N probes (where N is an odd integer) arranged symmetrically around the perimeter of a circle enable the first N-1 complex Fourier coefficients to be determined; addition of a probe at

the centre of the array gives the first 2N-1 complex coefficients.

The present study is concerned with a new method which has been developed for measuring directional spectra in greater detail than is possible with the "simple" types of gauge described in A. The method is suitable for situations in which the angular spread of wave energy does not exceed 180°, and therefore has potential for use at coastal sites. The equipment that is required is an array of waveheight-measuring probes arranged in a straight line perpendicular to the mean direction of wave propagation. The method of analysis is not based on the normal Fourier-series representation of the directional spectrum, but instead provides direct estimates of the angular distribution of the wave energy; it thereby avoids the problems associated with reconstructing a directional spectrum from a limited amount of data. This report describes the theory of the method and the results of tests which were carried out in the Offshore Sea Basin at HR to prove its validity.

2 THEORY OF LINEAR ARRAY

2.1 Principles

A right-handed co-ordinate system will be used in which the horizontal x,y plane coincides with the still-water surface and the z axis is taken vertically upwards. The direction of wave travel in the x,y plane is given by the angle θ which is measured anti-clockwise from the x-axis when viewed from above. A full list of symbols is given at the start of the report.

Consider a two-dimensional wave field whose statistical properties are homogeneous over the horizontal x,y plane. The directional nature of the waves can be described by a two-dimensional spectral density function $S_{II}(\omega, \theta)$ such that $S_{II}(\omega, \theta)\, d\omega\, d\theta$ is the energy of the waves having frequencies between ω ($= 2\pi/\text{period}$) and $\omega + d\omega$ and travelling in directions between θ and $\theta + d\theta$. The two-dimensional spectrum can be represented in the form

$$S_{II}(\omega, \theta) = S_I(\omega)\, f(\omega, \theta) \qquad (1)$$

where $S_I(\omega)$ is the one-dimensional frequency spectrum (as measured at a point) and $f(\omega, \theta)$ is an angular density function which, for a given frequency ω, describes how the energy of the waves varies with their direction θ. By definition it follows that

$$\int_0^{2\pi} S_{II}(\omega, \theta)\, d\theta = S_I(\omega) \qquad (2)$$

so that from equation (1)

$$\int_0^{2\pi} f(\omega, \theta)\, d\theta = 1 \qquad (3)$$

The wave field can be considered as the sum of a large number of elementary plane waves having surface elevations of the type

$$\eta = a \exp\left[i\,(kx \cos\theta + ky \sin\theta - \omega t + \phi)\right] \qquad (4)$$

where the wavenumber k (= 2π/wavelength) satisfies the linear dispersion relation

$$\omega^2 = gk \tanh kh \qquad (5)$$

in which h is the depth of the water. If the components of the wavenumber in the x and y directions are k_1 and k_2 respectively, so that

$$k_1 = k \cos\theta \qquad (6a)$$

$$k_2 = k \sin\theta \qquad (6b)$$

$$k^2 = k_1^2 + k_2^2 \qquad (6c)$$

then equation (4) can be written as

$$\eta = a \exp\left[i\,(k_1 x + k_2 y - \omega t + \phi)\right] \qquad (7)$$

Because of the inter-relationships between θ, ω, k_1 and k_2 it is possible to define the two-dimensional spectral density in several different ways. One version which will prove useful in the present study is $S_{II}(\omega, k_2)$, where k_2 is the component of the wavenumber in the y-direction. This function can be represented in the form

$$S_{II}(\omega, k_2) = S_I(\omega)\, g\,(\omega, k_2) \qquad (8)$$

where $g\,(\omega, k_2)$ is a spreading function which, for a given frequency ω, describes how the energy of the waves is distributed according to the wavenumber k_2. From equation (2) it follows that

$$\int_{-k}^{k} g(\omega, k_2)\, dk_2 = 1 \qquad (9)$$

The limits of the integration are equal to $\pm k$ because it is apparent from equation (6b) that k_2 cannot be greater than the wavenumber k. The relationship between the two types of spreading function, $f(\omega, \theta)$ and $g(\omega, k_2)$, can be found from the identity

$$S_{II}(\omega, \theta)\, d\omega\, d\theta = S_{II}(\omega, k_2)\, d\omega\, dk_2 \qquad (10)$$

which by means of equations (1), (6b) and (8) gives

$$g(\omega, k_2) = \frac{f(\omega, \theta)}{k \cos \theta} \qquad (11)$$

It should be noted here that normally $S_{II}(\omega, k_2)$ will only be a useful form of the two-dimensional spectrum if there are no waves travelling at angles of $|\theta| > \pi/2$. If such waves are present then energy at an angle $\pi - \theta$ cannot be distinguished from energy at an angle θ.

In A (Section 3.1) it was shown that if two output signals i and j are related by transfer functions F_i and F_j to an input signal with a spectrum $S(\omega, \alpha)$, then the cross-spectrum $S_{ij}(\omega)$ of the two output signals is given by

$$S_{ij}(\omega) = \int F_i^* F_j\, S(\omega, \alpha)\, d\alpha \qquad (12)$$

where * denotes the complex conjugate. Consider now a component wave of the type in equation (7) incident upon a pair of gauges at co-ordinate positions (x_o, y_o) and $(x_o, y_o + nd)$ so that nd is the horizontal distance between them; the waveheights measured by the gauges are

$$\eta_i = a \exp\left[i\,(k_1 x_o + k_2 y_o - \omega t + \phi)\right] \qquad (13a)$$

$$\eta_j = \eta_i \exp(i\, k_2\, nd) \qquad (13b)$$

Then from equations (12) and (13) it follows that the cross-spectrum of the signals from the two gauges, which are a distance nd apart, is

$$S_n(\omega) = \int_{-K}^{K} \exp(i\, k_2\, nd)\, S_{II}(\omega, k_2)\, dk_2 \qquad (14)$$

where the limits of the integration are such that

$$S_{II}(\omega, k_2) = 0 \quad \text{for} \quad |k_2| > K \qquad (15)$$

From equation (6b) it can be seen that K cannot be greater than the wavenumber k which depends upon the frequency of the waves and the depth of the water (see equation (5)).

Consider next an array of gauges arranged in a line parallel to the y-axis and positioned so as to give cross-spectra $S_n(\omega)$ for spacings of nd, where $n = 0, \pm (1, 2, \ldots\ldots, N-1)$. From equation (14) it follows that

$$S_{-n}(\omega) = S_n^*(\omega) \tag{16}$$

It will be shown shortly that estimates of the directional spreading function $g(\omega,k_2)$ can be obtained from the discrete transform

$$T_m(\omega) = \frac{1}{2N-1} \sum_{n=-(N-1)}^{n=N-1} S_n(\omega) \exp(-i\pi mn/N) \tag{17}$$

where the integer m serves to define particular values of k_2. From equation (17) it can be seen that

$$T_{m+2N}(\omega) = T_m(\omega) \tag{18}$$

so that distinct values of T_m are obtained for

$$-(N-1) < m < N \tag{19}$$

Substituting for $S_n(\omega)$ from equation (14) in equation (17) then gives

$$T_m(\omega) = \int_{-K}^{K} \frac{1}{2N-1} \sum_{n=-(N-1)}^{n=N-1} \exp\left[i\pi n\{(k_2 d/\pi)-(m/N)\}\right] \cdot S_{II}(\omega,k_2)\, dk_2 \tag{20}$$

Considering the quantity

$$P(X) = \frac{1}{2N-1} \sum_{n=-(N-1)}^{n=N-1} \exp(i\,2\pi nX) \tag{21}$$

it can be shown that

$$\left[\exp(i\pi X) - \exp(-i\pi X)\right] P(X) =$$

$$\frac{1}{2N-1} \left\{\exp\left[i(2N-1)\pi X\right] - \exp\left[-i(2N-1)\pi X\right]\right\} \tag{22}$$

which gives

$$P(X) = \frac{\sin\left[(2N-1)\pi X\right]}{(2N-1)\sin\left[\pi X\right]} \qquad (23)$$

The function P(X) is equal to unity at $X = 0, \pm(1, 2, \ldots\ldots)$ and has its first zeros at $X = \pm 1/(2N-1)$; the shape of the function for a value of N = 10 is shown in Fig 1. Thus equation (20) can be written as

$$T_m(\omega) = \int_{-K}^{K} P\left(\frac{k_2 d}{2\pi} - \frac{m}{2N}\right) S_{II}(\omega, k_2)\, dk_2 \qquad (24)$$

Using equation (8) then gives

$$\frac{T_m(\omega)}{S_I(\omega)} = \int_{-K}^{K} P\left(\frac{k_2 d}{2\pi} - \frac{m}{2N}\right) g(w, k_2)\, dk_2 \qquad (25)$$

which shows that the value of the quantity $T_m(\omega)/S_I(\omega)$ is the result of integrating the product of the spreading function $g(\omega, k_2)$ and the window function P(X); the integer m of the transform determines the value of k_2 about which the window function is centred, ie

$$k_2 = \frac{m\pi}{Nd} \qquad (26)$$

Since the window function P(X) is cyclic with a period of $\Delta X = 1$, aliasing effects can occur if the spreading function $g(\omega, k_2)$ extends over too great a range of wavenumbers. If the limits of k_2 are $\pm K$ (see equation (15)), aliasing will be avoided if

$$Kd < \pi \qquad (27)$$

2.2 Development

The theory described in 2.1 shows that the cross-spectra obtained from a linear array of gauges can be used to calculate a transform $T_m(\omega)$ (see equation (17)) whose value is related to the directional distribution of the wave energy. The nature of the relationship between the value of $T_m(\omega)$ and the spreading function $g(\omega, k_2)$ in equation (25) will now be studied.

Consider first the case of a directional sea which has a density function $g(\omega, k_2)$ that is rectangular in shape so that

$$g(\omega,k_2) = \begin{cases} D \text{ for } |k_2| < K \\ 0 \text{ for } |k_2| > K \end{cases} \tag{28}$$

From equation (9) it can be seen that

$$D = \frac{1}{2K} \tag{29}$$

Therefore equation (25) becomes

$$\frac{T_m(\omega)}{S_I(\omega)} = \frac{D}{r} \int_{-K}^{K} \frac{\sin ru}{\sin u} \, dk_2 \tag{30}$$

where $r = 2N-1$ (31a)
$u = (k_2 d-\alpha)/2$ (31b)
$\alpha = m\pi/N$ (31c)

Changing the variable of integration from k_2 to u gives

$$\frac{T_m(\omega)}{S_I(\omega)} = \frac{2D}{rd} \int_{U_1}^{U_2} \frac{\sin ru}{\sin u} \, du \tag{32}$$

where $U_1 = -(Kd + \alpha)/2$ (33a)
$U_2 = (Kd - \alpha)/2$ (33b)

Consider now the integral

$$I_r = \int \frac{\sin ru}{\sin u} \, du \tag{34}$$

Using the identity

$$\sin ru = \sin (r-1)u \cos u + \cos (r-1)u \sin u \tag{35}$$

twice and integrating shows that

$$I_r = I_{r-2} + \frac{2 \sin (r-1)u}{(r-1)} \tag{36}$$

Since r is always an odd integer (see equation (31a)), it follows that

$$I_r = u + \sum_{n=1}^{n=(r-1)/2} \frac{\sin 2nu}{n} \tag{37}$$

Substituting this result in equation (32) then gives

$$\frac{T_m(\omega)}{S_I(\omega)} = \frac{2DK}{(2N-1)} \left[1 + \frac{2}{Kd} \sum_{n=1}^{n=N-1} \frac{1}{n} \sin nKd \cos (nm\pi/N)\right] \tag{38}$$

Since the quantity on the right-hand side of this equation was not recognised as a series-type expansion of a standard function, its characteristics were studied by calculating numerical values. This showed that an estimator of the specified density function $g(\omega,k_2)$ in equation (28) at a value of

$$k_2 = \frac{m\pi}{Nd} \tag{39}$$

is given by the quantity

$$G_m = \frac{(2N-1)d}{2\pi} \frac{T_m(\omega)}{S_I(\omega)} \tag{40}$$

which from equation (38) is

$$G_m = D \frac{Kd}{\pi} \left[1 + \frac{2}{Kd} \sum_{n=1}^{n=N-1} \frac{1}{n} \sin nKd \cos (nm\pi/N)\right] \tag{41}$$

When $Kd = \pi$ (which corresponds to the aliasing limit in equation (27)), it can be seen that

$$G_m = D \tag{42}$$

for all values of m, so that the estimator reproduces the shape of the rectangular density function $g(\omega,k_2)$ exactly for values of $|k_2| < K$. When $Kd < \pi$ the estimator G_m differs a little from the specified rectangular distribution, but satisfactory results are obtained if N (the number of gauge spacings provided by the linear array) is sufficiently large; some typical results are shown in Fig 2.

A similar approach will now be used to study the case of a directional sea which has a density function $g(\omega,k_2)$ that is triangular in shape so that

$$g(\omega,k_2) = \begin{cases} E\left(1 - \frac{|k_2|}{K}\right) & \text{for } |k_2| < K \\ 0 & \text{for } |k_2| > K \end{cases} \tag{43}$$

From equation (9) it follows that

$$E = \frac{1}{K} \tag{44}$$

Substituting equation (43) in equation (25) gives

$$\frac{T_m(\omega)}{S_I(\omega)} = \frac{2E}{rd}\left(1 + \frac{\alpha}{Kd}\right)\int_{U_1}^{U_2} \frac{\sin ru}{\sin u}\,du - \frac{4E\alpha}{rKd^2}\int_{U_0}^{U_2} \frac{\sin ru}{\sin u}\,du$$

$$+ \frac{4E}{rKd^2}\int_{U_1}^{U_2} \frac{u \sin ru}{\sin u}\,du - \frac{8E}{rKd^2}\int_{U_0}^{U_2} \frac{u \sin ru}{\sin u}\,du \tag{45}$$

where r, u and α are given by equations (31a, b, c) respectively, and where

$$U_0 = -\frac{\alpha}{2} \tag{46}$$

and U_1 and U_2 are given by equations (33a, b) respectively. Consider now the integral

$$J_r = \int \frac{u \sin ru}{\sin u}\,du \tag{47}$$

Integrating by parts gives

$$J_r = u\, I_r - \int I_r\,du \tag{48}$$

where I_r is defined by equation (34). Making use of equation (37) for I_r then yields

$$J_r = \frac{u^2}{2} + \frac{1}{2n^2}\sum_{n=1}^{n=(r-1)/2}\left[2nu \sin 2nu + \cos 2nu\right] \tag{49}$$

Substituting these results for I_r and J_r in equation (45) gives after some lengthy manipulation

$$\frac{T_m(\omega)}{S_I(\omega)} = \frac{EK}{(2N-1)}\left[1 + \frac{4}{K^2D^2}\sum_{n=1}^{N-1}\frac{1}{n^2}(1 - \cos nKd).\right.$$

$$\left.\cos\,(nm\pi/N)\right] \tag{50}$$

In the previous case of a rectangular distribution it was found that the quantity G_m defined by equation (40) provided an estimate of the density function $g(\omega,k_2)$ at a value of $k_2 = m\pi/(Nd)$. In the present case of a triangular distribution the above result shows that G_m has the value

$$G_m = E \frac{Kd}{2\pi} \left[1 + \frac{4}{K^2D^2} \sum_{n=1}^{N-1} \frac{1}{n^2} (1 - \cos nKd) \cos (nm\pi/N)\right]$$

(51)

Representative calculations indicate that G_m in equation (51) gives a good estimate of the triangular density function $g(\omega,k_2)$ at a value of k_2 given by $k_2 = m\pi/(Nd)$; some typical results are shown in Fig 3.

The two examples considered above suggest that, in general, a satisfactory estimate of the spreading function $g(\omega,k_2)$ at a value of $k_2 = m\pi/(Nd)$ is provided by the quantity G_m in equation (40). G_m depends upon the discrete transform T_m defined by equation (17), so that the estimate of the spreading function is given by

$$g^1(\omega,k_2) = \frac{d}{2\pi S_I(\omega)} \sum_{n=-(N-1)}^{n=(N-1)} S_n(\omega) \exp(-i\pi nm/N) \quad (52)$$

where $S_I(\omega)$ is the one-dimensional energy spectrum and $S_n(\omega)$ is the cross-spectrum obtained from the linear array for a gauge spacing of nd. Normally it is more convenient to use the spreading function based on the wave direction θ rather than the one based on the wavenumber k_2. The relationship between $f(\omega,\theta)$ and $g(\omega,k_2)$ is given by equation (11), so that the estimate of the angular spreading function is

$$f^1(\omega,\theta) = \left[1 - \left(\frac{m\pi}{Nkd}\right)^2\right]^{\frac{1}{2}} \frac{kd}{2\pi S_I(\omega)} \sum_{n=-(N-1)}^{n=(N-1)} S_n(\omega) \cdot \exp(-i\pi nm/N) \quad (53)$$

where the integer m is related to the wave direction θ by

$$\theta = \sin^{-1}\left(\frac{m\pi}{Nkd}\right) \quad (54)$$

and the wavenumber k is a function of the frequency ω and the water depth h (see equation (5)). If the normalised version of the cross-spectrum $S_n(\omega)$ is represented as

$$\frac{S_n(\omega)}{S_I(\omega)} = C_n(\omega) + i\, Q_n(\omega) \quad (55)$$

and use is made of equation (16), than equation (53) can finally be expressed in the form

$$f^{1}(\omega,\theta) = \left[1 - \left(\frac{m\pi}{Nkd}\right)^{2}\right]^{\frac{1}{2}} \left(\frac{kd}{2\pi}\right) \cdot$$

$$\left\{1 + 2 \sum_{n=1}^{n=N-1} \left[C_n(\omega) \cos\left(nm\pi/N\right) + Q_n(\omega) \sin\left(nm\pi/N\right)\right]\right\} \qquad (56)$$

It is asumed here that the wave field is homogeneous so that $C_0(\omega) = 1$ and $Q_0(\omega) = 0$.

2.3 Application

The theory developed in the previous two sections enables estimates of the angular distribution of wave energy to be obtained from measurements of wave height made by a linear array of gauges. For best results the mean direction of wave propagation should be parallel to the x-axis and therefore perpendicular to the array (which is assumed to be parallel to the y-axis). As explained in Section 2.1 the array cannot differentiate between waves travelling at angles of θ and $\pi - \theta$, so that unambiguous results will be obtained only if there are no waves with directions $|\theta| > \pi/2$.

These conditions are satisfied in the case of a rectangular wave basin provided that the spending beach at the opposite end of the basin from the wave paddles absorbs the waves efficiently. The x-axis will now be taken to lie along the centreline of the basin and to be positive in the direction of wave travel; a positive angle θ of wave propagation is measured anti-clockwise from the x-axis when viewed from above (ie in the negative z-direction). The linear array is parallel to the y-axis and is therefore perpendicular to the centreline of the basin. The array does not have to be disposed symmetrically about the centre of the basin, but should be positioned in a part where the wave field is effectively homogeneous.

The theory does not specify the arrangement of the gauges in the linear array but only requires values of the cross-spectra $S_n(\omega)$ for a series of consecutive spacings

$$nd; \quad n = 0, \pm (1, 2, \ldots\ldots, N-1) \qquad (57)$$

It is therefore an interesting problem to determine the arrangement which will give the largest number of spacings for a given number of gauges. An upper limit is obtained by considering the possible combinations

of gauge pairs and assuming that there is no duplication of the spacings; for M gauges this gives the limit $N < 1 + M(M-1)/2$. However in practice it appears impossible to avoid some duplication of the spacings for arrays with more than four gauges. As yet no general principle has been found for determining the most efficient arrangements, and the best results obtained so far for arrays with up to nine gauges are shown in Fig 4.

After deciding upon the layout of the gauges within an array, it is necessary to choose a value for d, which is the unit dimension that determines the actual distances between the gauges. Normally d will be made as large as possible consistent with the need to avoid aliasing effects, which from equation (27) requires that $d < \pi/K$, where K is the limit of k_2 beyond which there is no wave energy (see equation (15)). The value of K cannot exceed that of the wavenumber k which increases as the frequency ω of the waves increases (see equation (5)). For measurements in the open sea the unit distance d is therefore determined by the maximum frequency of the waves which it is required to measure and by their likely directions relative to the linear array. In a wave basin a lower limit on the value of K may be set by the characteristics of the wave generators.

A computer program (called LINAR) has been developed to analyse measurements from a linear array of wave-height gauges. The program is written in a general way so that, with sufficient storage limits, it can deal with any number of gauges in any specified arrangement. The first step in the calculations is to carry out a Fourier analysis of each channel of data using the Fast Fourier Transform technique described by Thompson and Gilbert [5]. Estimates of the frequency spectra of each channel (ie $S_{ii}(\omega)$ in equation (12)) and of the cross-spectra between pairs of channels (ie $S_{ij}(\omega)$) are then obtained by suitably multiplying the complex Fourier coefficients and averaging them within equally-spaced frequency bands. It should be noted here that the cross-spectrum $S_{ij}(\omega)$ corresponds to $S_n(\omega)$ in equation (14) provided that signal i is given by a gauge at co-ordinate position $y = y_o$ and signal j by a gauge at $y = y_o + nd$; if the positions of the gauges were reversed, $S_{ij}(\omega)$ would correspond to $S_{-n}(\omega)$.

The theoretical analysis assumes that all the gauges in an array will give equal values of the one-dimensional spectrum $S_I(\omega)$. In practice this is unlikely to happen because, even if the wave field were truly homogeneous, statistical variations would still occur due to the finite number of data samples. The computer program makes two types of allowance for

this effect. When calculating the one-dimensional spectrum $S_I(\omega)$, the overall value is found from the formula

$$S_I(\omega) = \frac{1}{M} \sum_{i=1}^{i=M} S_{ii}(\omega) \qquad (58)$$

where M is the number of gauges in the array. However, when calculating the normalised cross-spectral values $C_n(\omega)$ and $Q_n(\omega)$ for use in equation (56), it is better to disregard equation (55) and use values given by

$$C_n(\omega) + i\, Q_n(\omega) = \frac{S_{ij}(\omega)}{\left[S_{ii}(\omega)\, S_{jj}(\omega)\right]^{\frac{1}{2}}} \qquad (59)$$

where i and j denote the pair of gauges which are separated by a distance of nd. If the array contains more than one pair of gauges with this spacing, then the arithmetic mean of the quantity on the right-hand side of equation (59) is used to calculate $C_n(\omega)$ and $Q_n(\omega)$.

An interesting feature of this new theory is that the directional resolution of the linear array varies with the frequency of the waves. This can be contrasted with the "simple" types of gauge (see Section 1) which make use of a Fourier-series representation of the directional spectrum; with these gauges the number of terms that can be evaluated depends only upon how many separate channels of information are measured. In the case of the linear array direct estimates of the spreading function $f(\omega, \theta)$ are obtained from equation (56) by varying the integer m which, via equation (54), also determines the corresponding wave direction θ. If θ is relatively small the angle $\Delta\theta$ between successive estimates of $f(\omega, \theta)$ is given approximately by

$$\Delta\theta = \frac{\pi}{Nkd} \qquad (60)$$

Use of equation (5) gives for waves in deep water

$$\Delta\theta = \frac{g\pi}{N\omega^2 d} \qquad (61)$$

which illustrates the dependence of the angular resolution on the wave frequency ω. Although the transform T_m in equation (17) can be calculated for

values of the integer m between -(N-1) and N-1, equation (56) shows that valid results for the spreading function $f(\omega, \theta)$ are only obtained if m does not exceed the limit

$$|m| < \frac{Nkd}{\pi} \qquad (62)$$

Thus it follows that the number of estimates of $f(\omega, \theta)$ given by the linear array increases as the frequency of the waves increases.

3 EXPERIMENTS

3.1 Equipment

Tests on two types of linear array have been carried out at HR in the Offshore Sea Basin (OSB) which measures 25m x 25m in plan and has a normal water depth of 2.0m. Waves are generated by 80 hinged paddles arranged in a continuous line along one wall of the basin. The basin can produce short-crested random waves with most types of angular distribution, as well as long-crested random and regular waves.

The first array consisted of 5 HR twin-wire resistance gauges, each 600mm long, arranged in the layout shown in e of Fig 4. The unit spacing, which determines the actual distances between the gauges, was chosen as d = 0.40m; this gave an overall length for the array of 3.6m. The meniscus which surface tension produces around a wire has practically no effect on the output of a resistance-type gauge, but the calibration is affected by changes in the conductivity of the water. The calibration factor of each gauge was therefore determined once a day by moving the gauge through a known vertical distance in still water and measuring the change in output voltage. The calibrations were found to be accurately linear, and readings were repeatable to within about ± 0.5mm.

The second array consisted of 9 capacitance gauges arranged according to the layout shown in i of Fig 4. The unit spacing was kept at d = 0.40m so that the overall length of the array was 11.6m. The capacitance probes are of a new HR design, and are 600mm long with a diameter of 3.5mm which includes an FEP (fluoroethylenepropylene) water-repellent sheathing. An advantage of this type of gauge is that its calibration is unaffected by changes in the conductivity of the water. This saves time when carrying out measurements because the gauges need only be calibrated once, and this can be done before they are installed in the array. Also the mounting arrangements for capacitance gauges are simpler because, unlike resistance gauges, there is no need to

move them up and down in the water. However a disadvantage of capacitance gauges is that the measurements can be adversely affected by meniscus problems.

Preliminary tests to compare the performance of a resistance gauge and a capacitance gauge were carried out in the OSB by making simultaneous recordings of various regular and random waves. In regular waves with a frequency of 0.4Hz the resistance gauge indicated larger wave heights than the capacitance gauge (by about 5mm or 2.5% of the actual wave-height). However at a frequency of 1.0Hz the situation was reversed, and the capacitance gauge then gave the larger values (by about 5-10mm or 3-6% of the actual wave height). Comparison of the measured wave profiles showed that those from the capacitance gauge were less sinusoidal in shape and were more flattened at the peaks than those from the resistance gauge. When tested in random seas, with peak frequencies ranging from 0.42Hz to 0.80Hz, it was found that the capacitance gauge gave spectral densities that were on average 8% lower near the peak of the spectrum than those from the resistance gauge. However, the results also indicated that the capacitance gauge produced more noise at higher frequencies, so that overall the signals from the two gauges had approximately equal energies.

In summary these results suggest that the capacitance gauge is less accurate than the resistance gauge, and that the discrepancies are mainly due to meniscus effects. Thus an array of resistance gauges is likely to give better estimates of the one-dimensional spectrum $S_I(\omega)$ than a similar array of capacitance gauges. However, the differences in the estimates of the angular spreading function $f(\omega, \theta)$ may be smaller because some of the errors due to meniscus effects will tend to cancel out when normalised values of the cross-spectra are calculated for use in equation (56).

3.2 Measurements

The arrays were tested in the OSB and were mounted on a bridge spanning the basin; the method of attachment allowed the arrays to be moved in both the longitudinal and transverse directions. However, the comparison tests were carried out with the arrays symmetrically disposed about a point near the centre of the basin.

Each array was used to measure the four directional spectra listed in Table 1; the fifth spectrum, which was long-crested, was measured only with the 9-gauge array. These spectra cover the normal range of operating conditions in the OSB and were also used in

the previous study described in A. The short-crested seas produced by the wave paddles were specified to have angular spreading functions of the type

$$f(\omega, \theta) = \begin{cases} \frac{1}{A_n} \cos^n \theta; & |\theta| < \pi/2 \\ 0 & ; \quad |\theta| > \pi/2 \end{cases} \tag{63}$$

with the mean direction of propagation being parallel to the centreline of the basin. In each spectrum the same spreading function was applied over the whole range of generated frequencies. From equation (3) it follows that

$$A_n = \int_{-\pi/2}^{\pi/2} \cos^n \theta \, d\theta \tag{64}$$

Integrating by parts yields the reduction formula

$$A_n = \frac{(n-1)}{n} A_{n-2} \tag{65}$$

Thus if n is an even iteger

$$A_n = \left[\frac{(n-1)\ (n-3)\ \ldots\ 1}{n\ (n-2)\ \ldots\ 2}\right]\pi \tag{66}$$

while if n is odd

$$A_n = \left[\frac{(n-1)\ (n-3)\ \ldots\ 2}{n\ (n-2)\ \ldots\ 1}\right]2 \tag{67}$$

Therefore, for a $\cos^2\theta$ distribution $A_2 = \pi/2$, and for a $\cos^6\theta$ distribution $A_6 = 5\pi/16$.

In the tests, recordings were normally made about ten minutes after the wave paddles were started in order to allow time for any initial disturbances to die away. In each run 4096 samples of waveheight data were recorded from each of the 5 or 9 gauges in the linear array. The measurements were recorded by computer and each scan of the data channels was carried out nearly instantaneously. The intervals between the scans depended upon the characteristics of the spectra and are given in Table 1.

4 RESULTS

The wave measurements obtained from the linear arrays were analysed using the program LINAR described in Section 2.3. The 4096 samples from each data channel

were used to calculate spectral estimates at the centres of 32 frequency bands, with each estimate representing the average of 64 Fourier coefficients.

Average values of the one-dimensional spectrum $S_I(\omega)$ were calculated from equation (58), and the results from the two arrays are compared with the specified spectra in Figs 5 a-e. The plots show that there is generally good agreement between the measured and specified spectra. Comparing the results from the two arrays, it can be seen that on average the capacitance gauges give smaller spectral values then the resistance gauges near the peak of each spectrum, but larger values at the high-frequency end. This behaviour is in accordance with the findings of the preliminary tests described in Section 3.1. However, the differences are not very large, and the performance of both types of gauge would normally be quite acceptable.

The estimates of the angular spreading function given by the 5-gauge array are shown in Figs 6 a-d and by the 9-gauge array in Figs 7 a-e. As explained in Section 2.3, the angular intervals between the estimates depend upon the number of gauges in the array and become smaller as the frequency increases. In each plot results for 4 frequencies near the peak of the spectrum have been superimposed. Figs 6 a-d for the array of 5 resistance gauges show that in general the estimated values of the spreading function agree well with the specified values, particularly for the $\cos^6\theta$ distribution. The differences are largest at $\theta = 0$, where in most cases the measured wave energies are lower than specified. The reason for these discrepancies has not yet been identified, but may be connected with the method of wave generation rather than with the system of measurement. However, viewed overall, the results confirm the validity of the measurement technique, and also show that the basin does produce waves with the required directional distributions.

Comparison of Figs 6 a-d and 7 a-d shows that the results from the array of 9 capacitance gauges are more scattered than those from the 5-gauge array. This is partly because the 9-gauge array provides about three times as many values so that each estimate is smoothed over a smaller angular range. However, some of the differences may also be due to the lower accuracy of the capacitance gauges (see 3.1) which would tend to increase the amount of noise in the results.

An interesting indication of the resolving power of the linear array is provided by Fig 7e which shows the measurements obtained from the 9-gauge array for the

long-crested spectrum LMMA. Theoretically the spreading function for this spectrum should appear as an infinitely high spike at $\theta = 0$, but when viewed by the array some of this concentrated energy will be spread over angles either side of zero. Also it is difficult in practice to generate perfect long-crested waves because their height is affected by cross-waves and other disturbances in the basin. The results in Fig 7e are therefore encouraging because they demonstrate that the measuring technique can resolve a single spike, and that in the case of the 9-gauge array the spreading of the energy is limited to an angular band approximately 10° wide.

The accuracy and resolution of a linear array depends upon the number of gauges used, the unit spacing d and of course the performance of the gauges themselves. In the present study the 5-gauge array gave only a few angular estimates at low frequencies, while at higher frequencies the 9-gauge one tended to provide a surfeit of information. The angular resolution can be increased by enlarging the unit spacing d (see equation (60)), and Figs 2 and 3 show that this also improves the accuracy of the individual estimates. However, it is necessary to avoid the aliasing limit given by equation (27), and in the laboratory tests the figure of d = 0.4m was based on the maximum value of K that could be generated; if accurate results had only been required for frequencies below 1.1Hz, it would have been possible to increase d to 0.6m.

The present study suggests that a 6-gauge array should normally provide a sufficient amount of directional information. Consider the requirements for a linear array installed at a coastal site having a water depth of 20m. The larger the unit spacing d, the finer the angular resolution, but a limit on the size of d is provided by equation (27); if the required angular range is ± 90°, then equation (27) is equivalent to

$$d < \lambda/2 \qquad (68)$$

where λ is the wavelength of the waves. If the shortest waves to be measured have a period of 6 seconds, then it can be shown from equations (5) and (68) that the unit spacing d needs to be less than about 27m. Choosing, for example, d = 20m would result in a 6-gauge array with an overall length of 260m. The angular resolution is determined approximately from equation (60), and for 6 second waves it would be about 6° and for 16 seconds about 24°. Although the waveheights were measured in the laboratory by surface-piercing gauges, the theory could be adapted for use with bottom-mounted pressure gauges.

5 CONCLUSIONS

A new method of measuring directional wave spectra by means of a linear array of waveheight gauges has been developed and tested successfully. The technique is suitable for use at coastal sites provided that the angular spread of wave energy does not exceed 180°. Detailed conclusions are:

(1) The linear array has the important advantage of providing direct estimates of the angular distribution of wave energy. Most other methods use a Fourier series representation of the directional spectrum, and suffer from poor angular resolution when the spectrum is reconstructed from a limited number of terms.

(2) The angular resolution of such an array depends upon the number of gauges and the distances between them, and also varies with the frequency of the waves.

(3) The method was tested in the Offshore Sea Basin at HR using one array with 5 resistance gauges and another with 9 capacitance gauges. Satisfactory agreement was found between the directional spectra generated in the basin and those measured by the two arrays.

(4) The laboratory experiments suggest that a 6-gauge array should normally provide a satisfactory amount of directional information. At a coastal site with a 20m depth of water an array with a unit spacing of d = 20m would have an angular resolution of about 6° for waves with a 6 second period and about 24° for waves with a 16 second period. Waveheights could be measured by surface-piercing gauges or by bottom-mounted pressure gauges.

6 ACKNOWLEDGEMENTS

This study was carried out in the Offshore Group of the Maritime Engineering Department headed by Dr S W Huntington.

The concept and basic principles of the linear array were originated by Mr G Gilbert, and the experimental measurements were made by Mr C J Malinowski. Design of the capacitance wave gauges was the responsibility of Mr D K Fryer, and development and testing were carried out by Mr L J Smith and Mr M W S Thomas.

7 REFERENCES

1. CAPON J High-resolution frequency-wave number spectrum analysis. Proc of IEEE, Vol 57, No 8, Aug 1969, pp 1408-1418.

2. CARTWRIGHT D E and SMITH N D Buoy techniques for obtaining directional wave spectra. Buoy Technology, Marine Tech Soc, 1964, pp 112-121.

3. GILBERT G Directional spectra by Maximum Likelihood. Hydraulics Research Station, Tech note, 1978.

4. MAY R W P Measurement of mean direction and spread of wave spectra. Hydraulics Research Limited, Report IT 247, April 1983.

5. THOMPSON D M and GILBERT G The Fast Fourier Transform with applications to spectral and cross-spectral analysis. Hydraulics Research Station, Report INT 100, Dec 1971.

DDB Dd 650449 4/85

Table

TABLE 1

TEST SPECTRA: SPECIFIED CHARACTERISTICS

SPECTRUM NAME	TYPE	PEAK FREQUENCY Hz	ANGULAR DISTRIBUTION	SIGNIFICANT WAVEHEIGHT metres	SCANNING INTERVAL seconds
SSPJ2	JONSWAP	0.42	$\cos^2\theta$	0.150	0.300
SJMED	JONSWAP	0.55	$\cos^2\theta$	0.155	0.227
SSPM2	MOSKOWITZ	0.80	$\cos^2\theta$	0.061	0.157
SSPM6	MOSKOWITZ	0.80	$\cos^6\theta$	0.061	0.157
LMMA	MOSKOWITZ	0.60	LONG-CRESTED	0.107	0.208

Figures

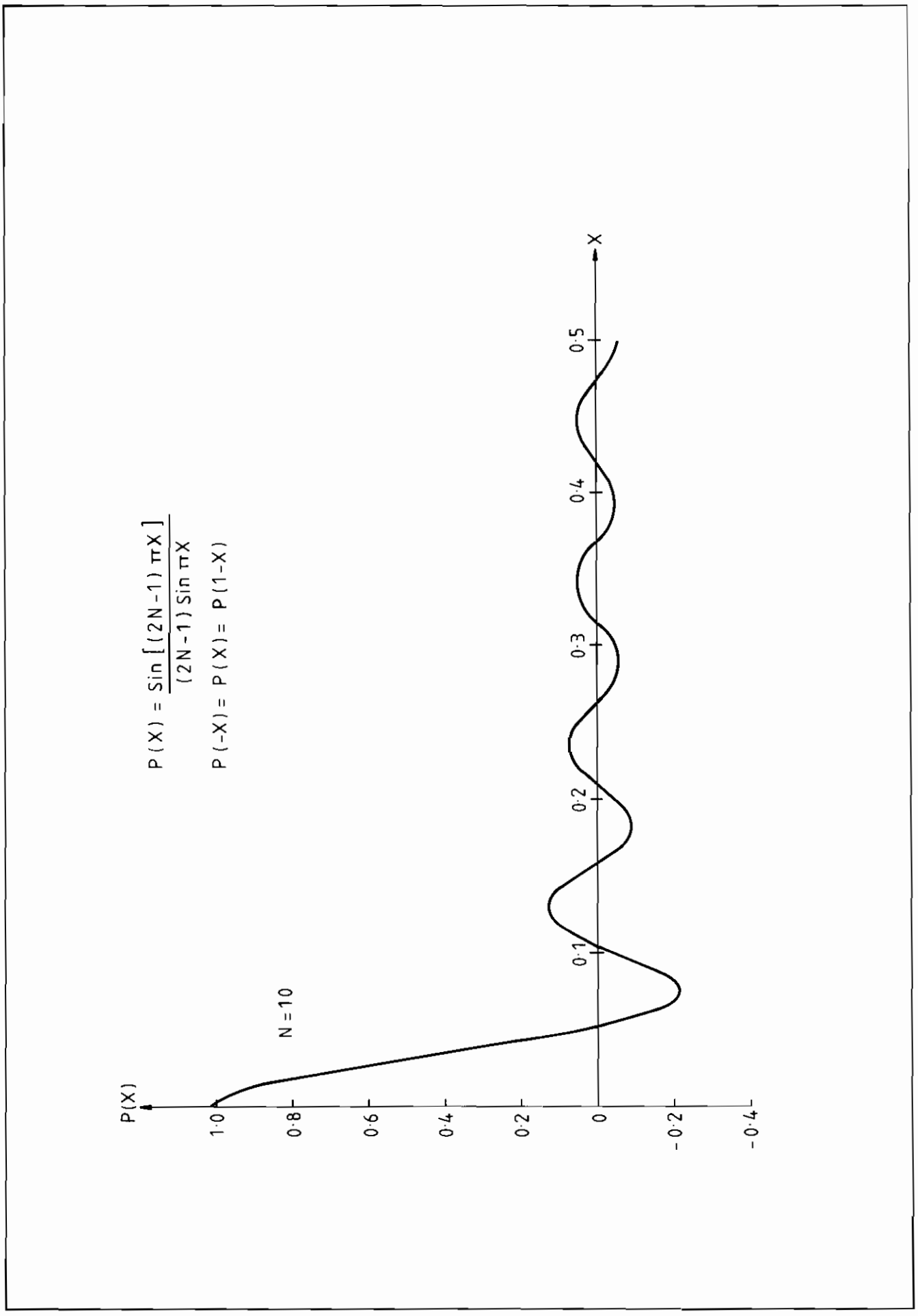

Fig 1 Function P(X)

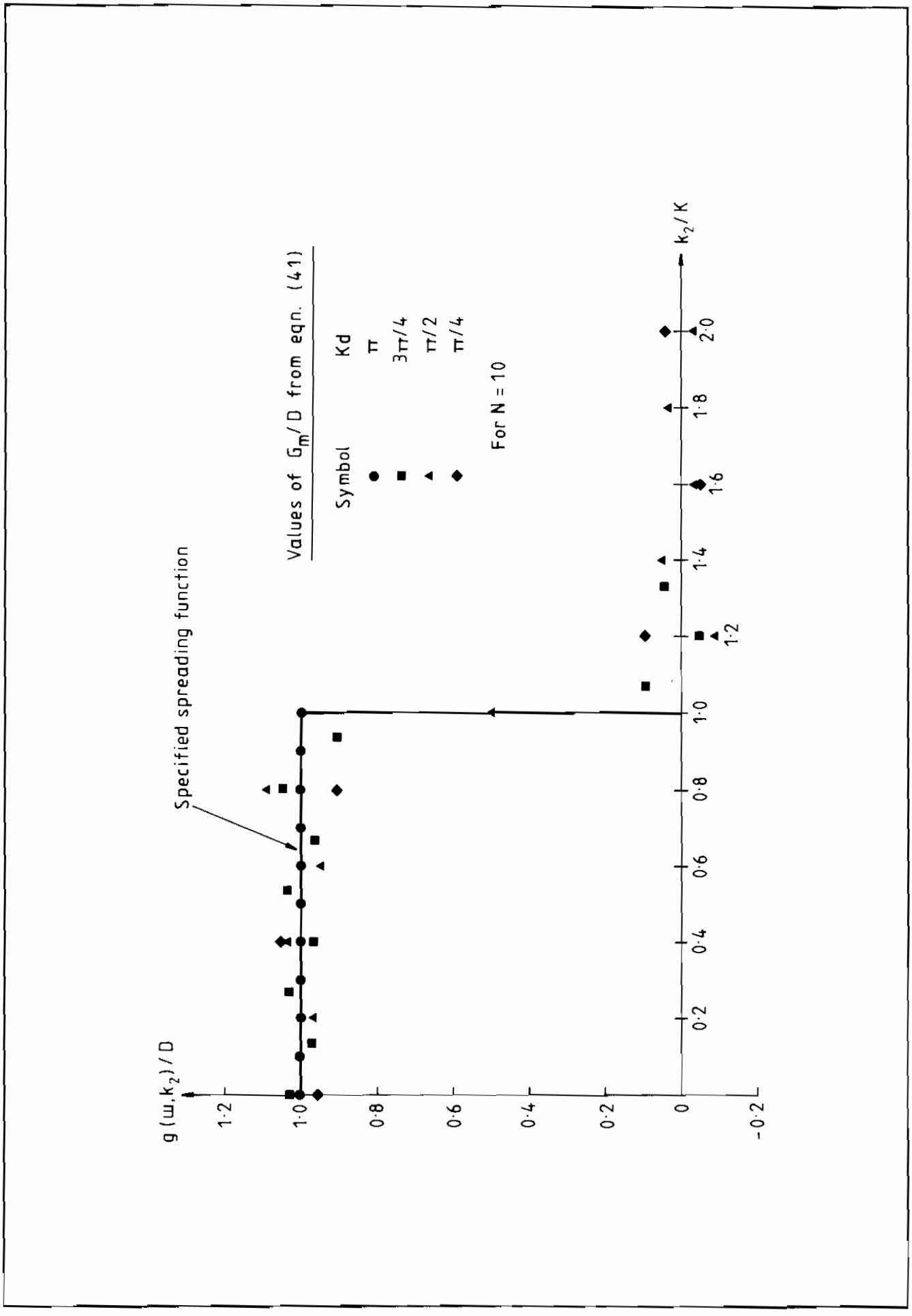

Fig 2 Estimated values of rectangular spreading function

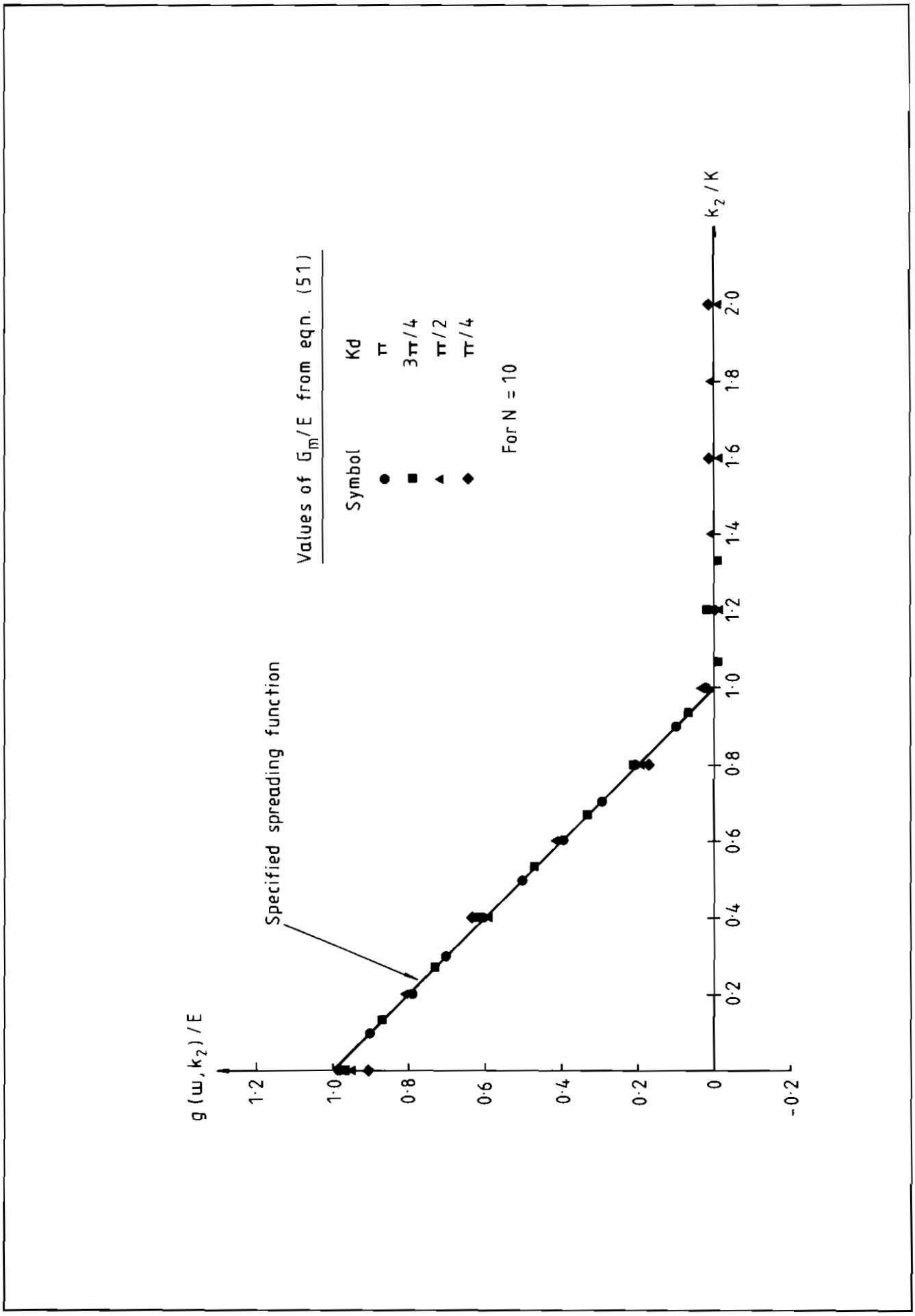

Fig 3 Estimated values of triangular spreading function

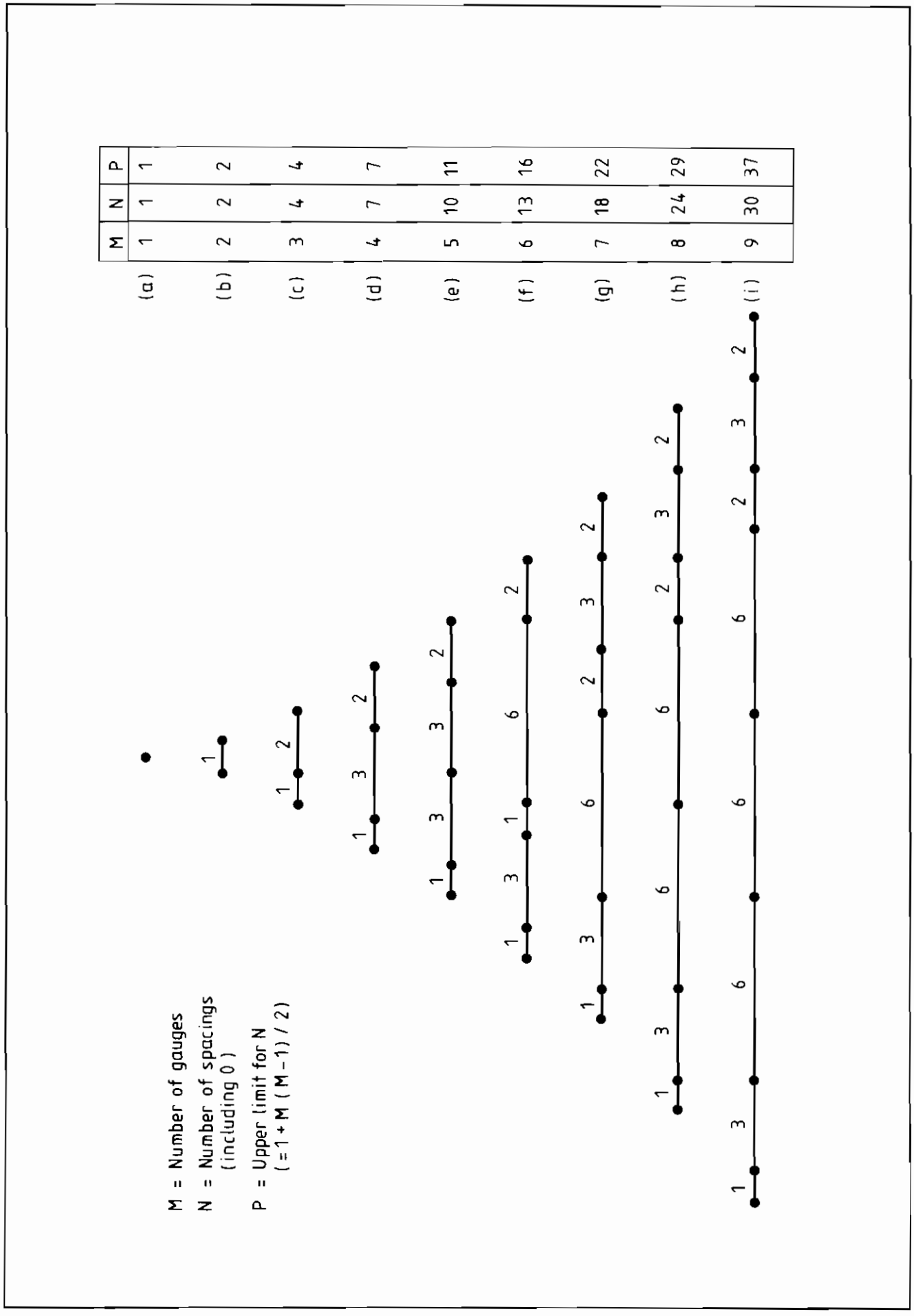

	M	N	P
(a)	1	1	1
(b)	2	2	2
(c)	3	4	4
(d)	4	7	7
(e)	5	10	11
(f)	6	13	16
(g)	7	18	22
(h)	8	24	29
(i)	9	30	37

Fig 4 Arrangements of gauges in linear array

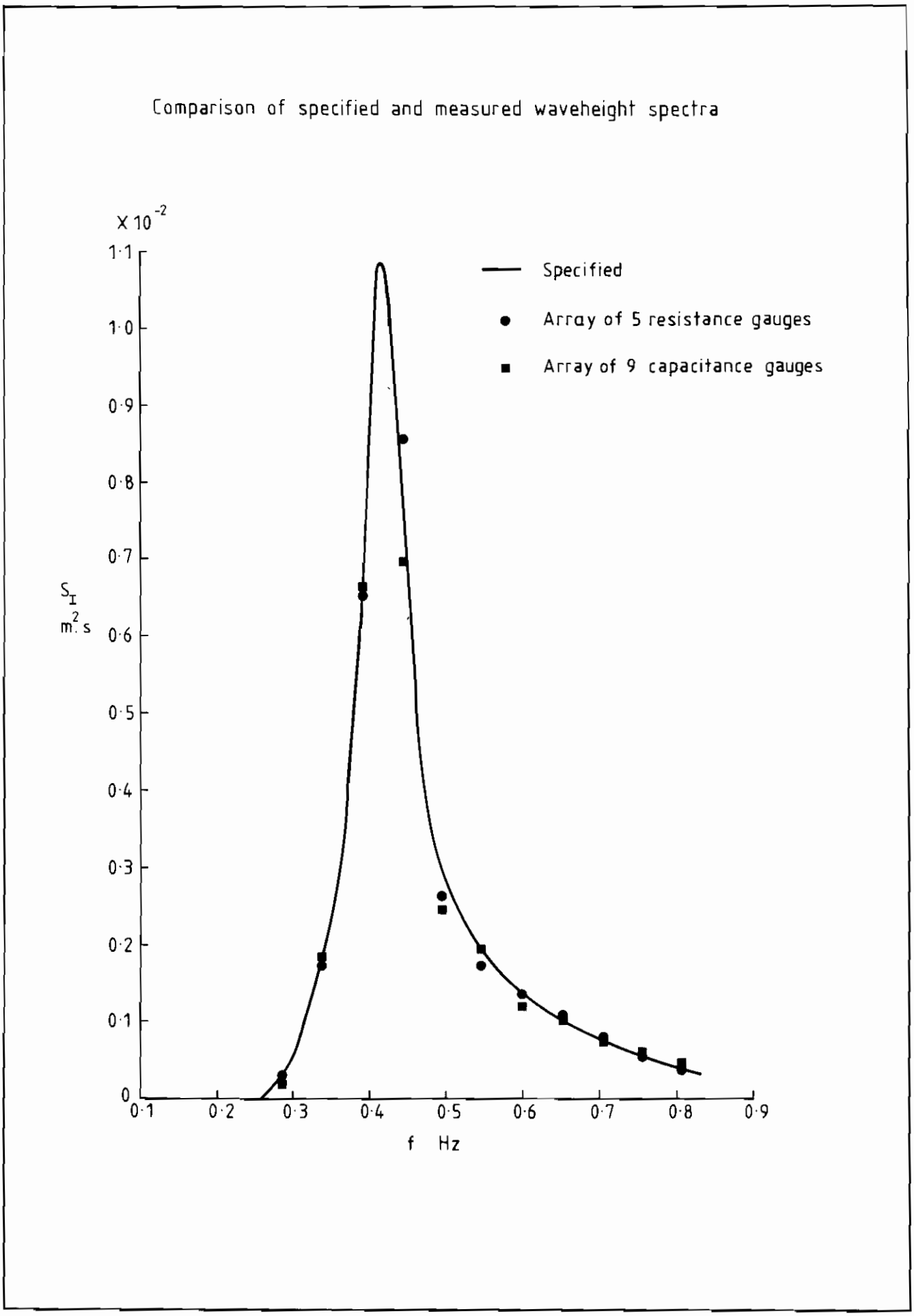

Fig 5a Spectrum SSPJ2

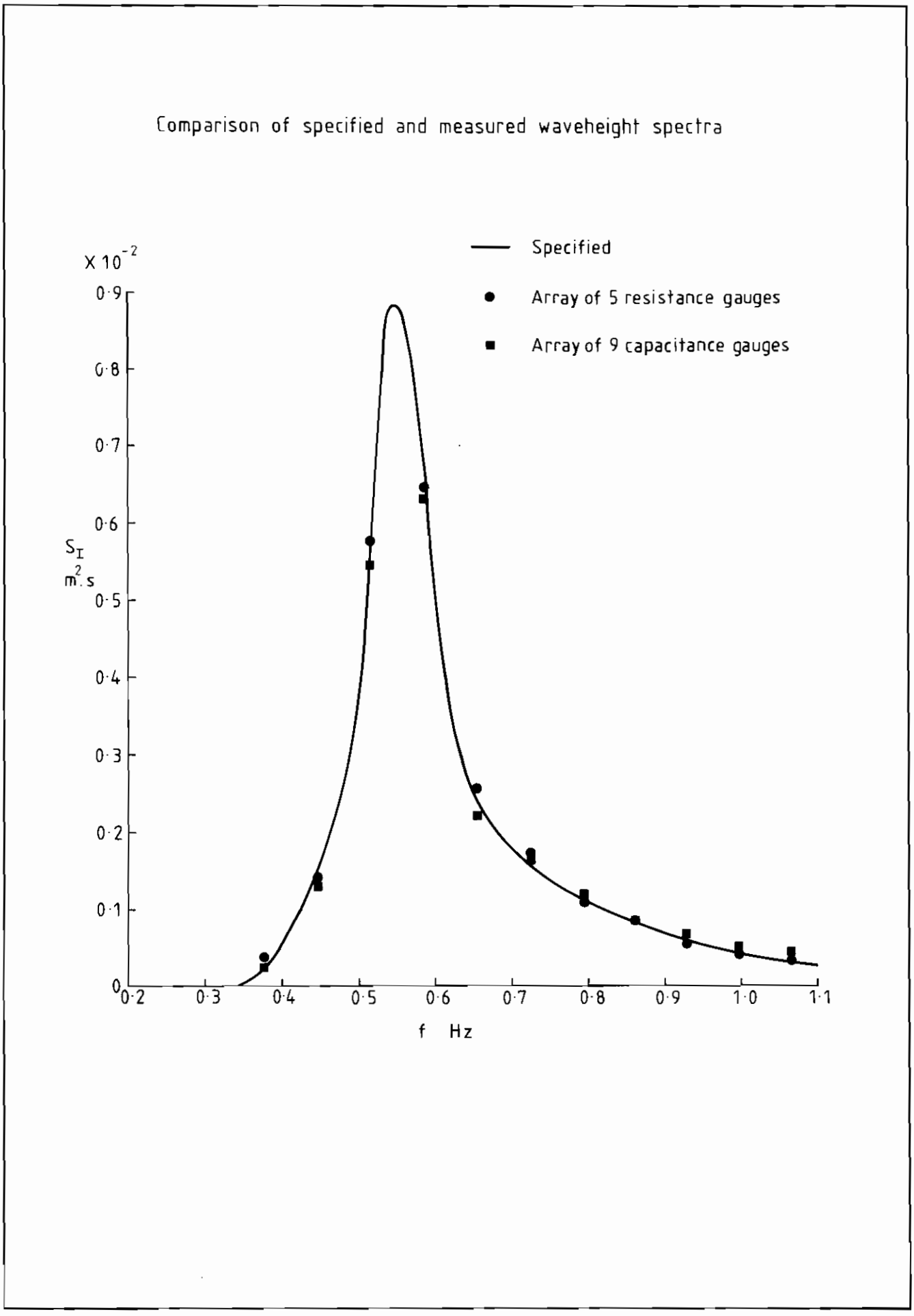

Fig 5b Spectrum SJMED

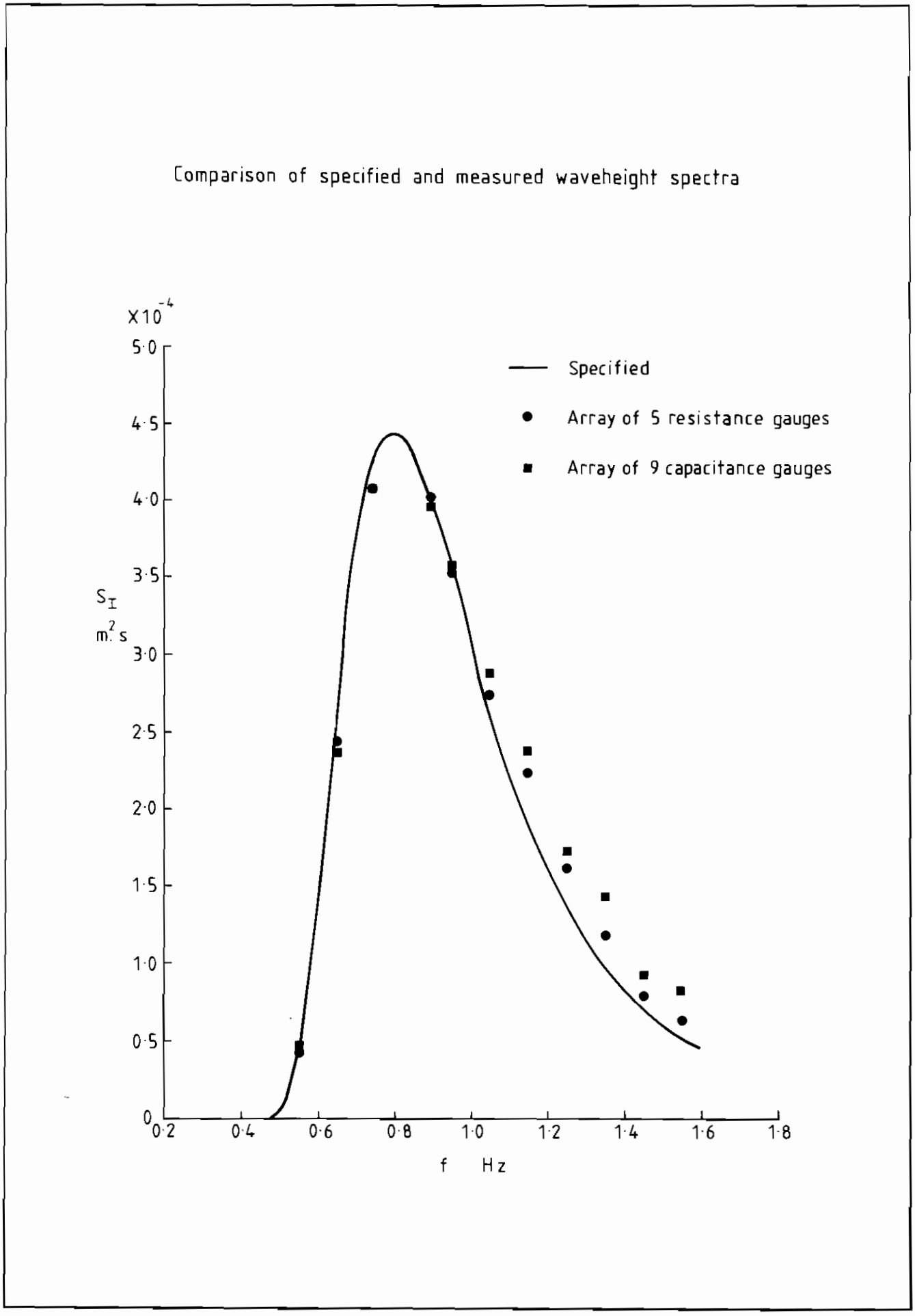

Fig 5c Spectrum SSPM2

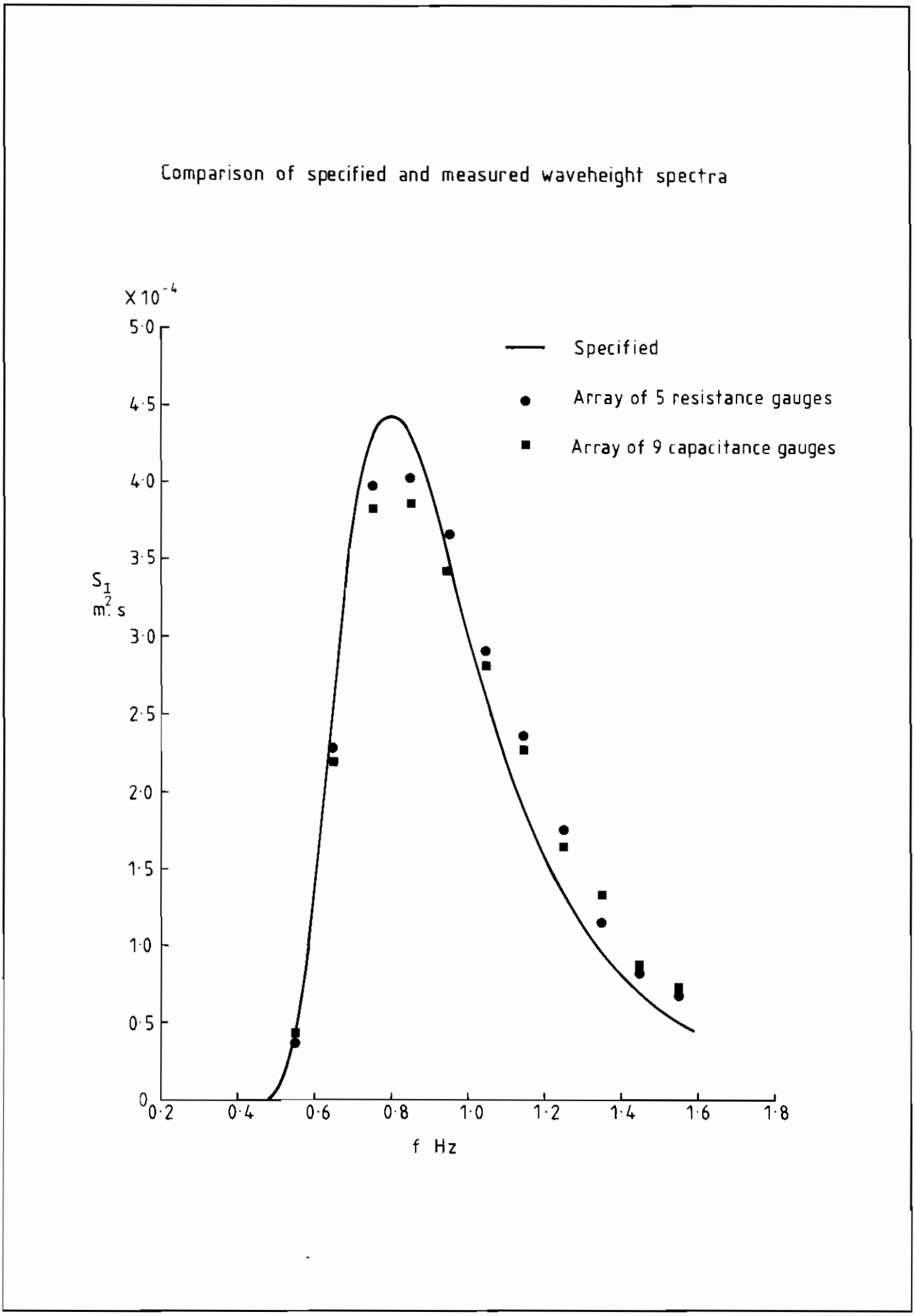

Fig 5d Spectrum SSPM6

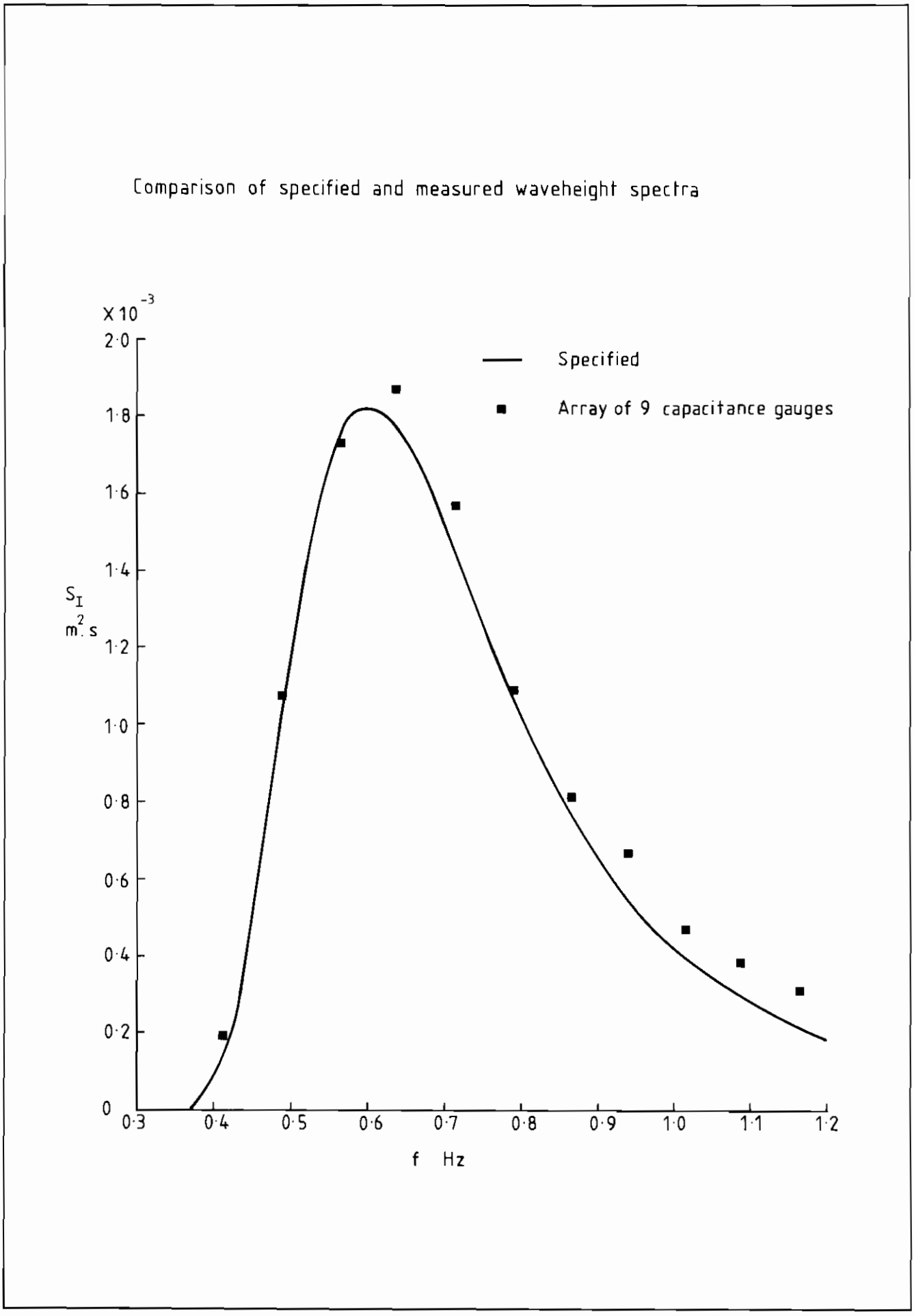

Fig 5e Spectrum LMMA

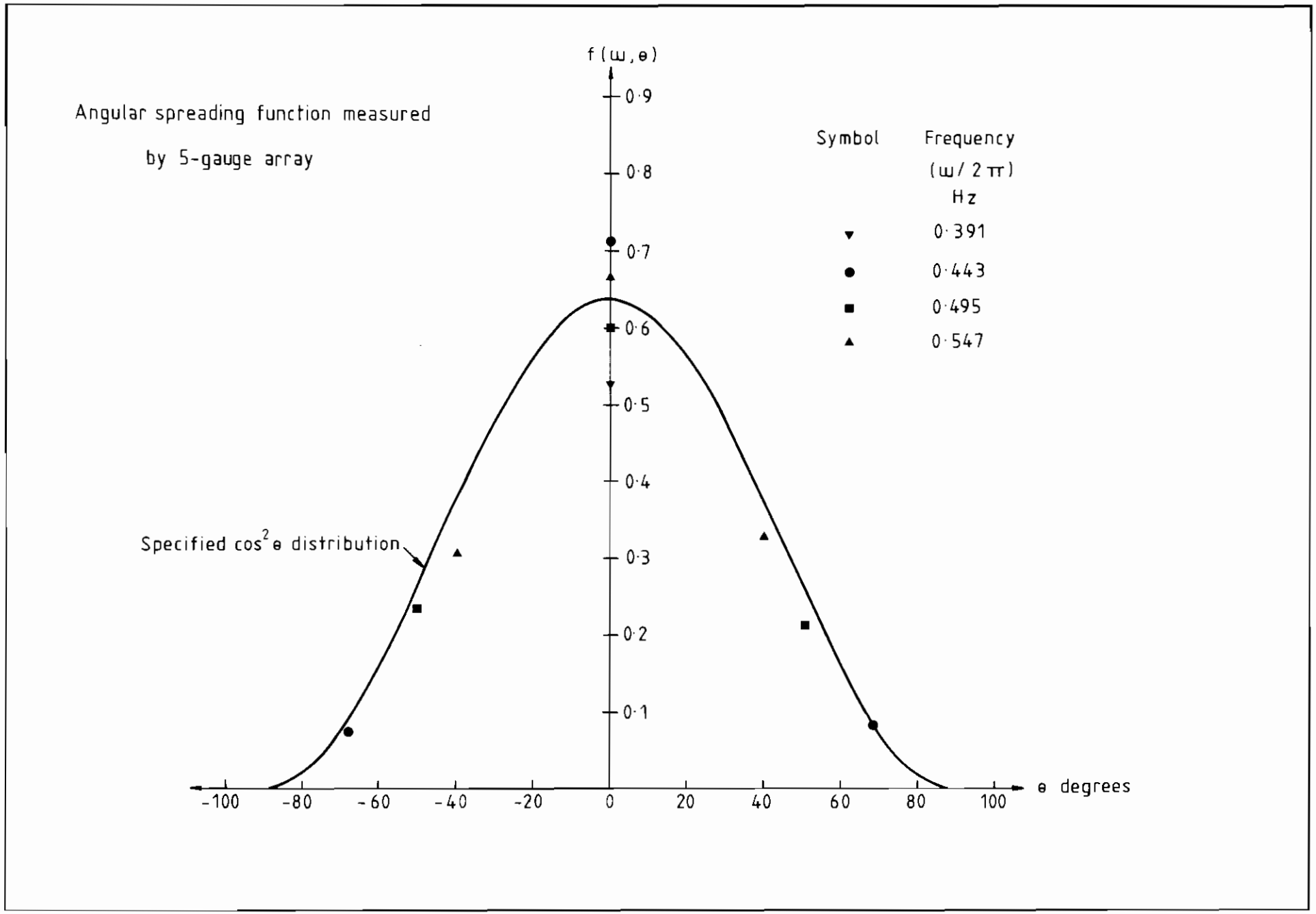

Fig 6a Spectrum SSPJ2

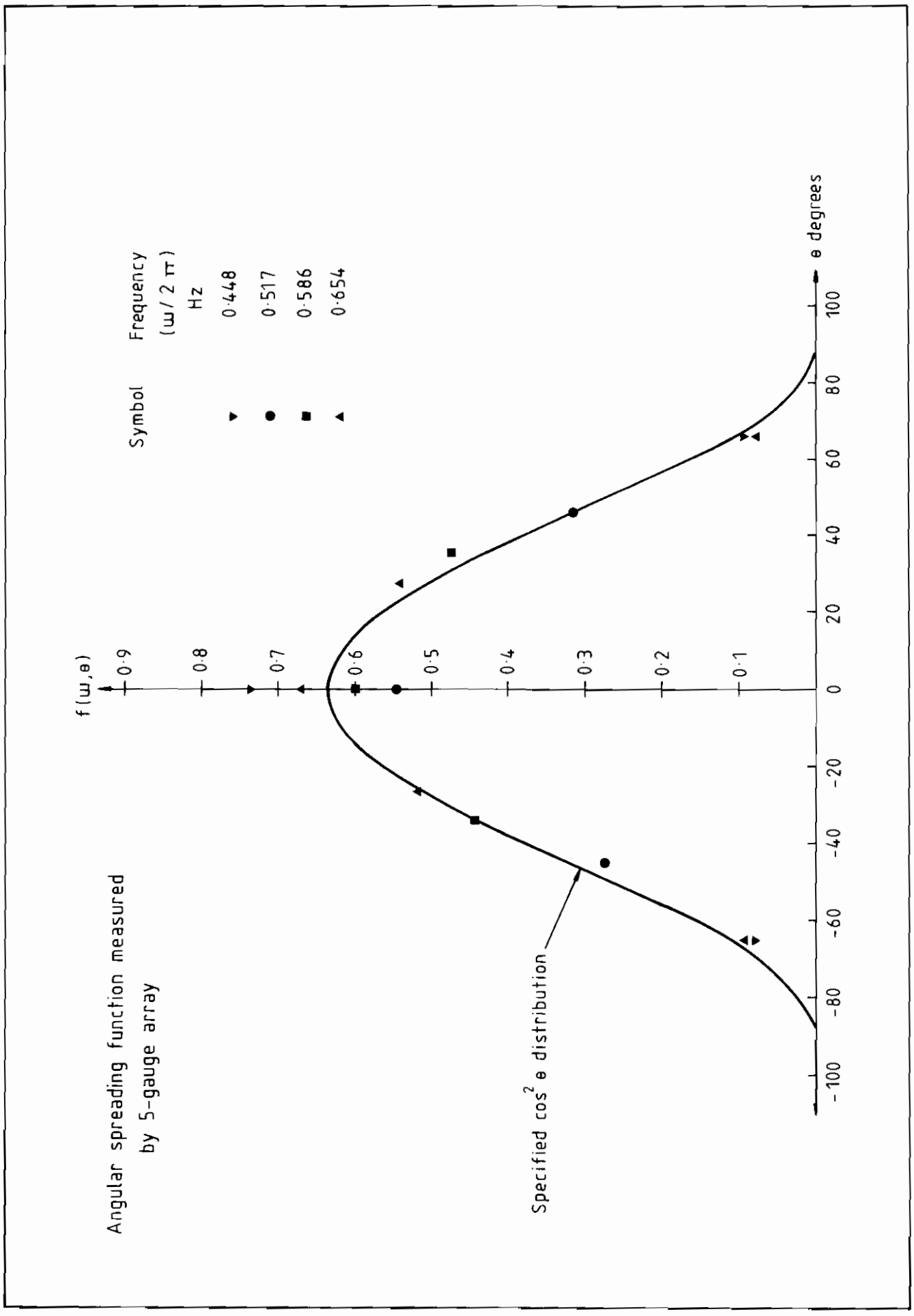

Fig 6b Spectrum SJMED

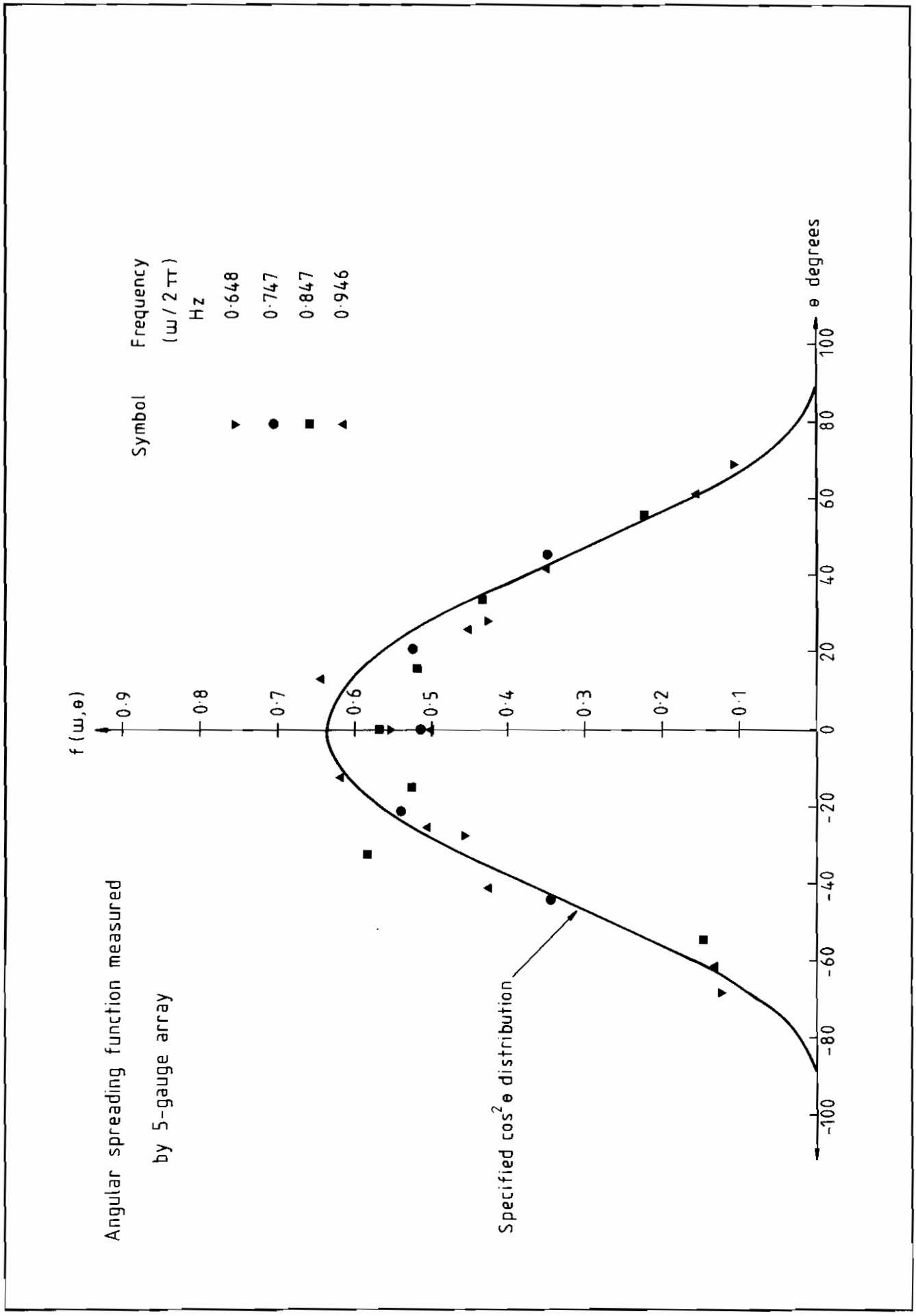

Fig 6c Spectrum SSPM2

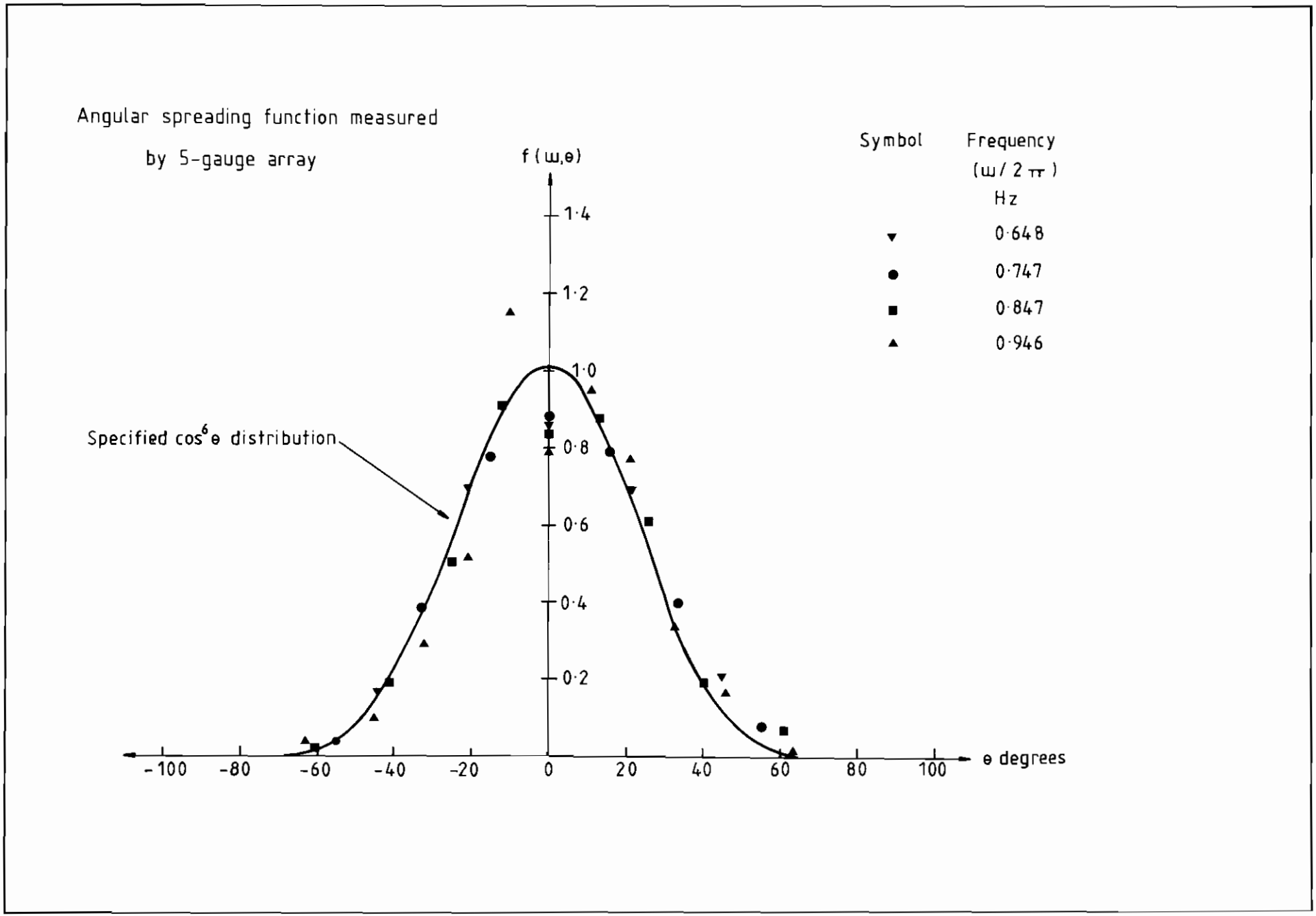

Fig 6d Spectrum SSPM6

Fig 7a Spectrum SSPJ2

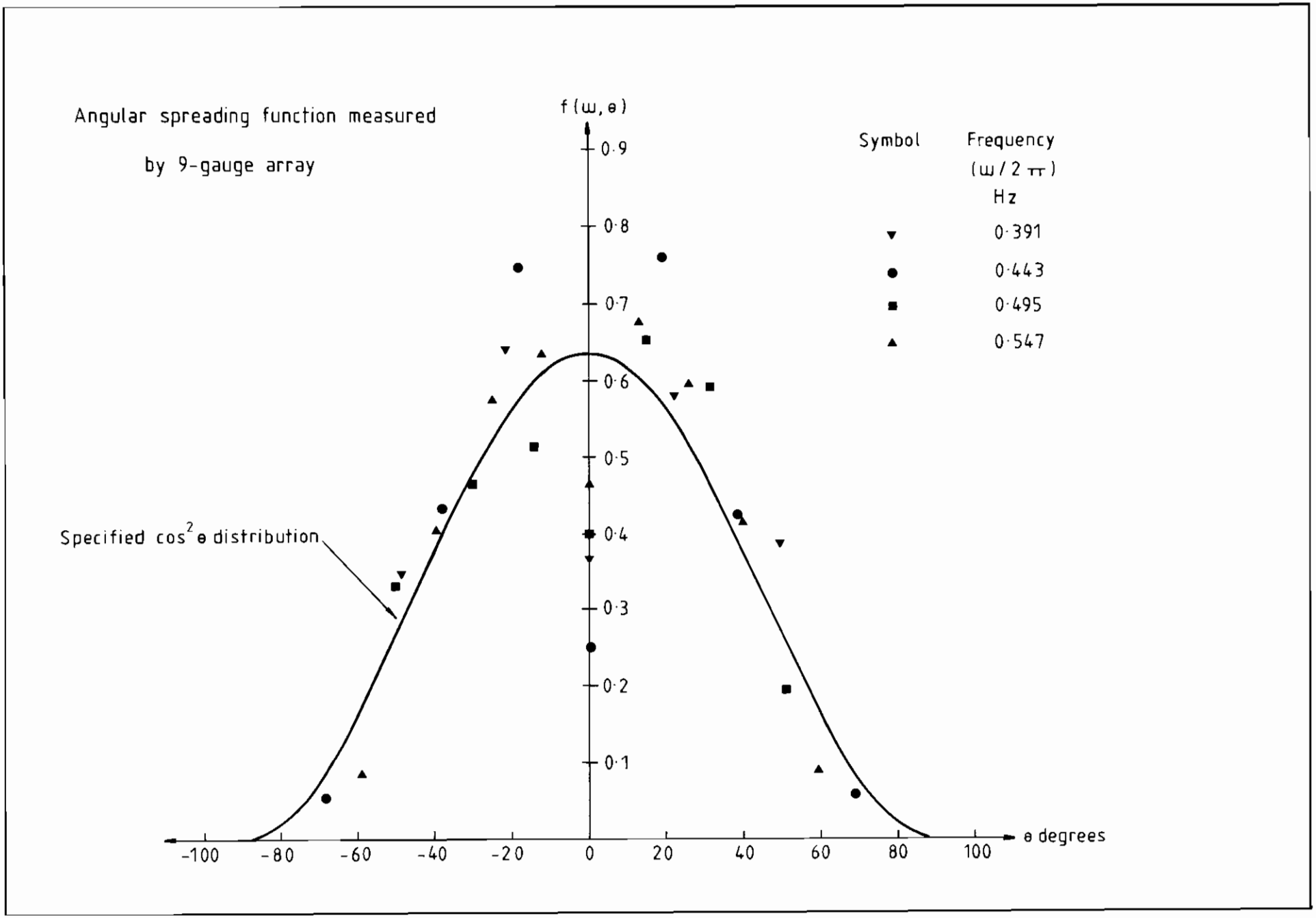

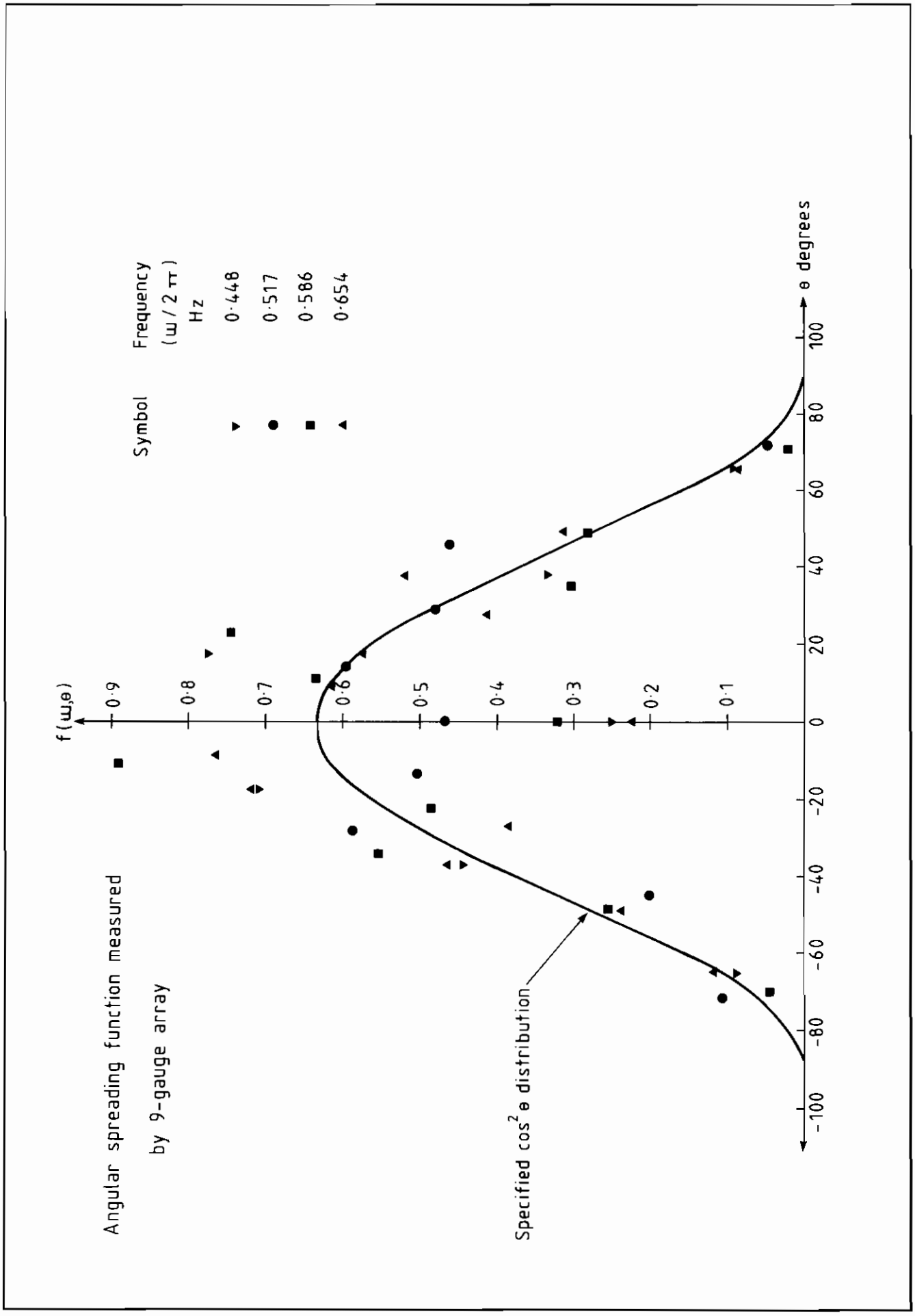

Fig 7b Spectrum SJMED

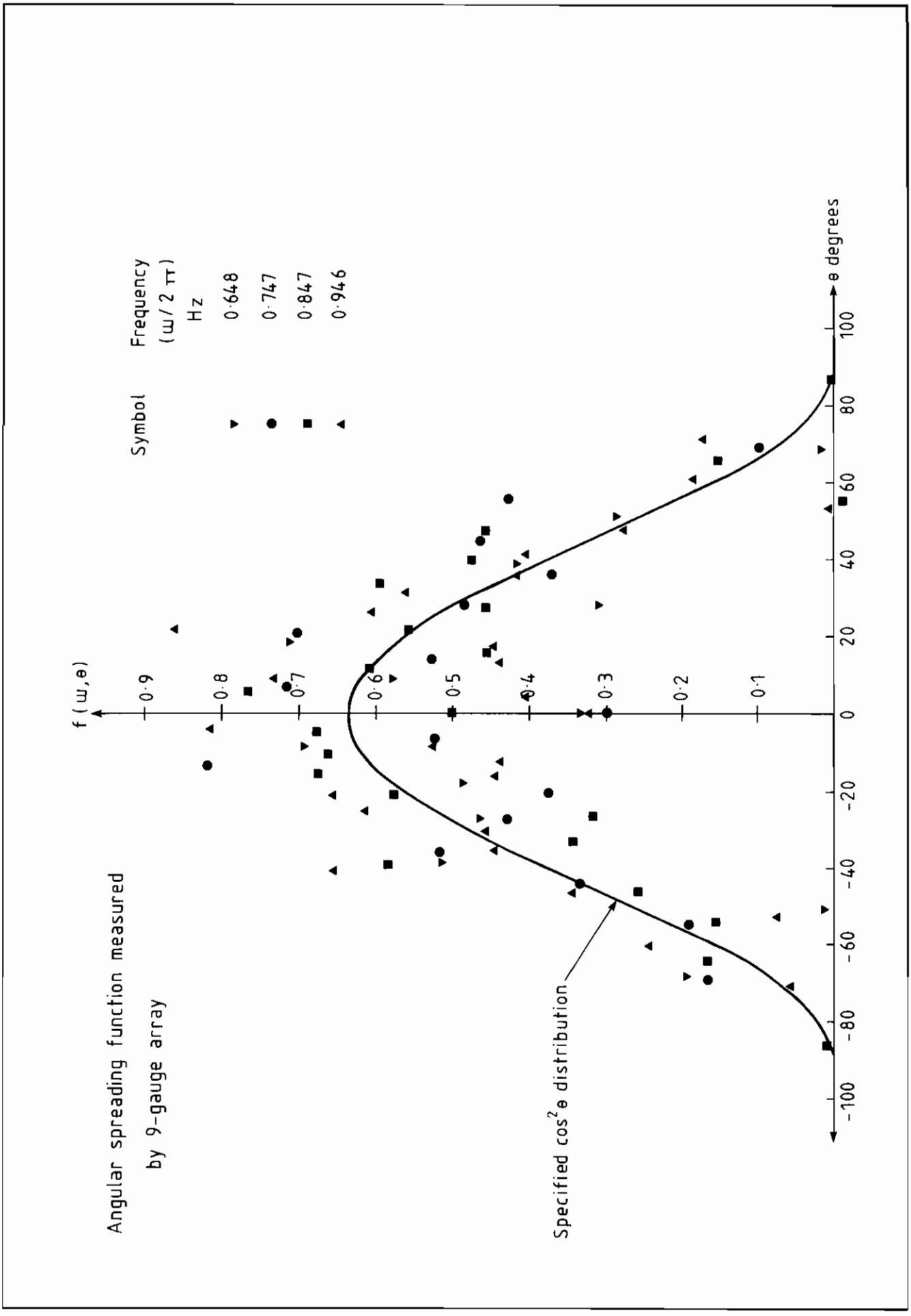

Fig 7c Spectrum SSPM2

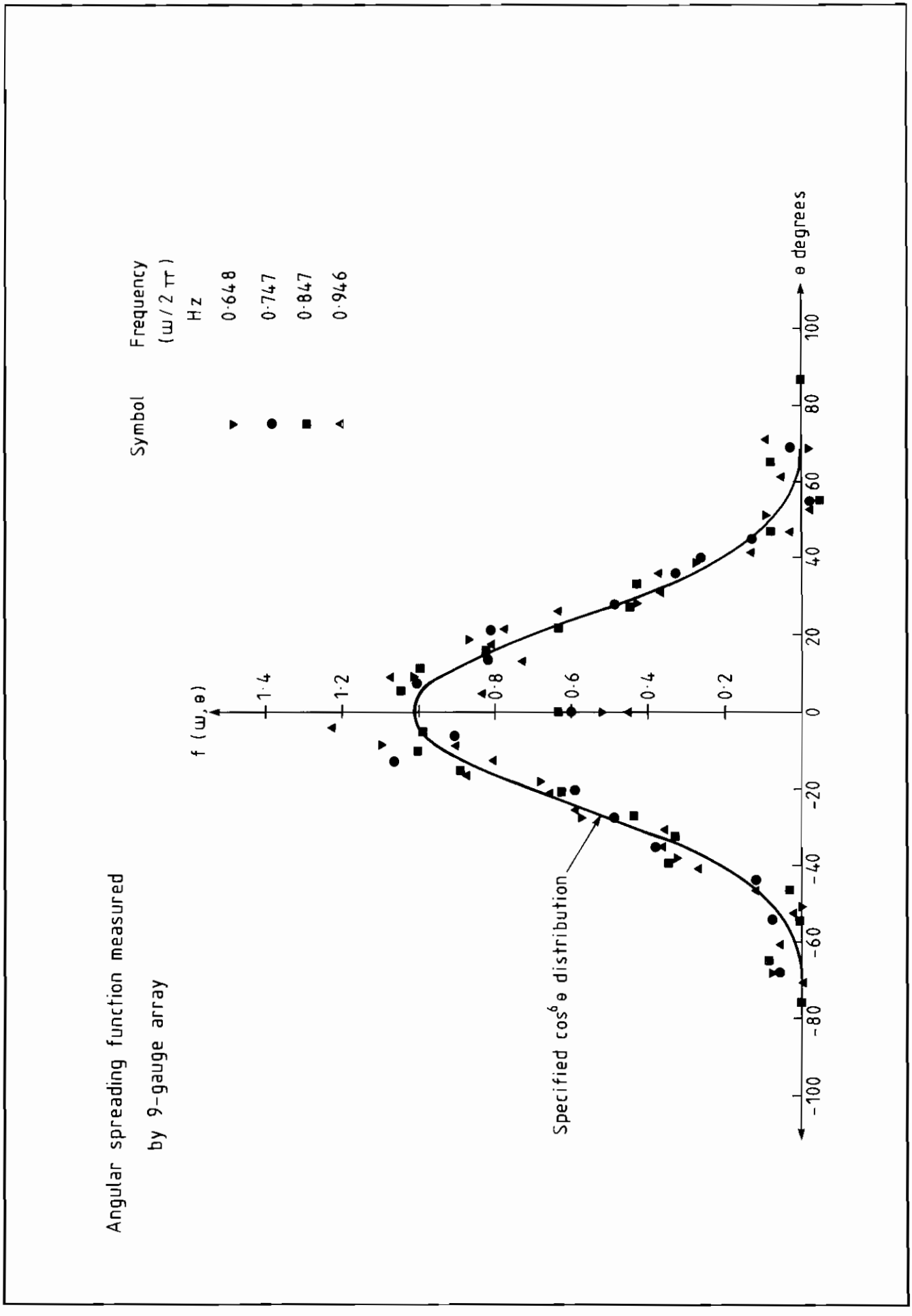

Fig 7d Spectrum SSPM 6

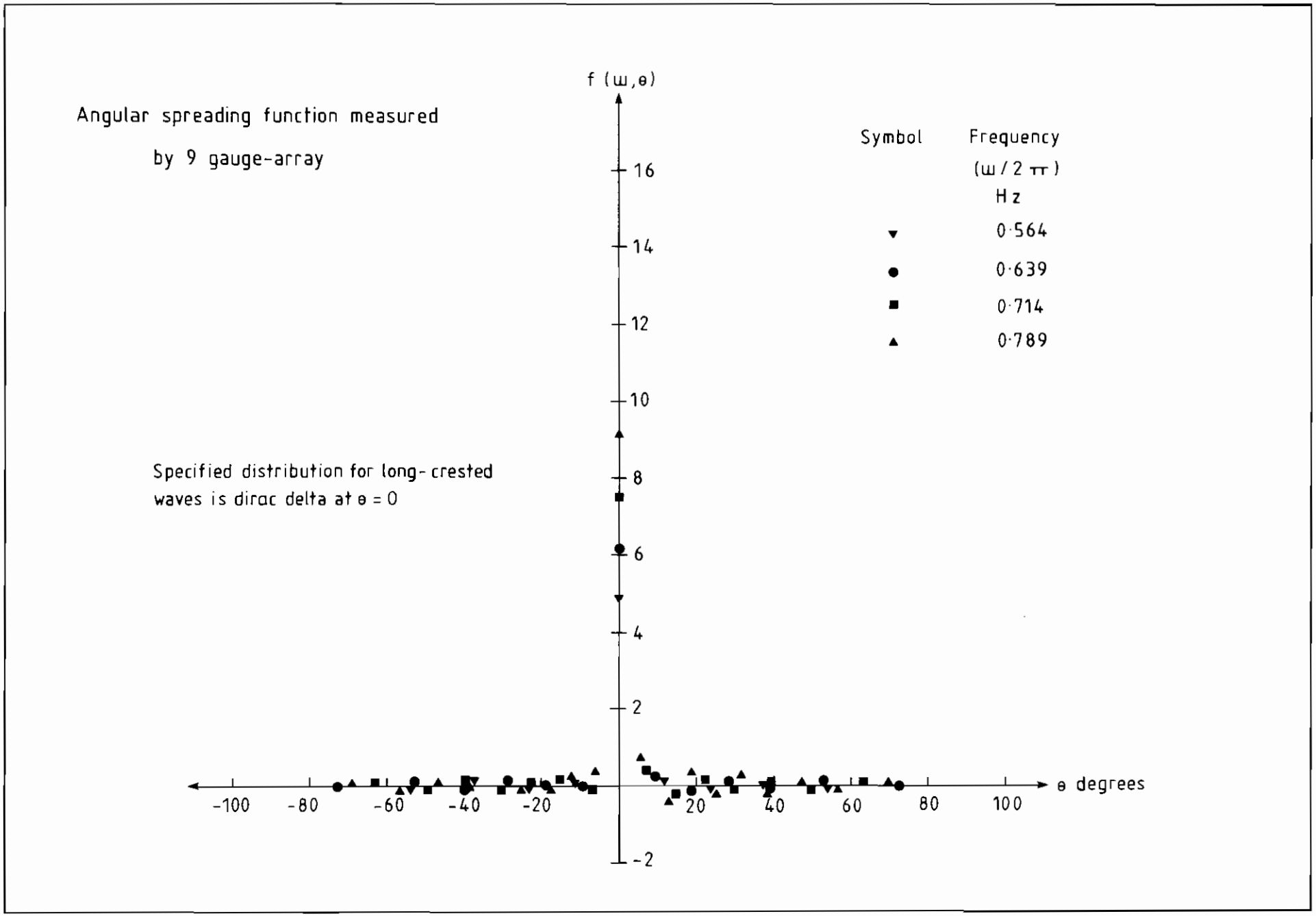

Fig 7e Spectrum LMMA